

Joint Transmit and Pinching Beamforming for PASS: Optimization-Based or Learning-Based?

Xiaoxia Xu, Xidong Mu, Yuanwei Liu, *Fellow, IEEE*, and Arumugam Nallanathan, *Fellow, IEEE*

Abstract—A novel pinching antenna system (PASS)-enabled downlink multi-user multiple-input single-output (MISO) framework is proposed. PASS consists of multiple waveguides spanning over thousands of wavelength, which equip numerous low-cost dielectric particles, named pinching antennas (PAs), to radiate signals into free space. The positions of PAs can be reconfigured to change both the large-scale path losses and phases of signals, thus facilitating the novel *pinching beamforming* design. A sum rate maximization problem is formulated, which jointly optimizes the transmit and pinching beamforming to adaptively achieve constructive signal enhancement and destructive interference mitigation. To solve this highly coupled and nonconvex problem, both optimization-based and learning-based methods are proposed. 1) For the optimization-based method, a majorization-minimization and penalty dual decomposition (MM-PDD) algorithm is developed, which handles the nonconvex complex exponential component using a Lipschitz surrogate function and then invokes PDD for problem decoupling. 2) For the learning-based method, a novel Karush-Kuhn-Tucker (KKT)-guided dual learning (KDL) approach is proposed, which enables KKT solutions to be reconstructed in a data-driven manner by learning dual variables. Following this idea, a KDL-Tranformer algorithm is developed, which captures both inter-PA/inter-user dependencies and channel-state-information (CSI)-beamforming dependencies by attention mechanisms. Simulation results demonstrate that: i) The proposed PASS framework significantly outperforms conventional massive multiple input multiple output (MIMO) system even with a few PAs. ii) The proposed KDL-Tranformer can improve over 30% system performance than MM-PDD algorithm, while achieving a millisecond-level response on modern GPUs.

Index Terms—Beamforming, deep learning, flexible antennas, pinching antenna system (PASS), pinching beamforming.

I. INTRODUCTION

Shannon's theorem establishes the capacity upper bound of wireless communication systems based on the signal-to-noise (SNR) ratio [1], which dramatically depends on channel qualities of mobile users. To break through the limitation of fixed-channel assumptions and make radio environment customizable, recent advances in sixth-generation (6G) wireless networks have been devoted to developing several new forms of flexible-antenna techniques, such as reconfigurable intelligent surfaces (RISs) [2], [3], fluid antennas [4], and movable antennas [5]. Specifically, RISs equip a large amount of low-cost passive reflective/transmissive meta-material elements to reconfigure the communication environment by altering the

phase shifts and amplitudes of incident signals [2], [3]. More recently, fluid antenna and movable antenna systems have been proposed [4], [5], which enable the transceivers/receivers to dynamically adjust antenna positions and their electromagnetic properties, thus creating favorable spatial channels for multi-input multi-output (MIMO) communications.

Despite the promises, there are two limitations of existing flexible-antenna techniques. On the one hand, the transceivers/receivers typically spans across a restricted spatial range, which significantly limits their capabilities to reconfigure large-scale path loss and maintain stable line-of-sight (LoS) links for mobile users. Particularly, in RISs-aided systems, the received signals typically undergo the channel fading of both the base station (BS)-RIS links and the RIS-user links. Moreover, fluid antennas and movable antennas usually move within a few wavelengths, which lead to minor effects on the large-scale path loss and suffer from susceptibility to barrier blockage in high-frequency communications. On the other hand, existing flexible-antenna techniques are usually equipped with a fixed number of antennas, which are difficult to flexibly scale up/down according to realistic demands.

To circumvent these drawbacks, pinching antenna system (PASS) has recently emerged as a novel flexible-antenna technique [6], [7]. PASS is built on a rod-like transmission line, named dielectric waveguide, whose length spans from a few meters to tens of meters, and even up to thousands of times longer than the wavelength [8]. The dielectric waveguide acts as a leaky-wave antenna, where multiple radiation points, implemented by *dielectric particles*, can be flexibly pinched and released anywhere along this waveguide. These small *dielectric particles* are known as pinching antennas (PAs), which enables radio-wave transmission and reception of PASS. Amongst existing flexible antenna techniques, PASS has several unique advantages [7]: 1) *Path-loss reconfiguration and LoS link construction*: PASS can reconfigure the large-scale path loss to deliver wireless services to the last-meter range, and maintain stable LoS links to avoid blockage in high-frequency communications. 2) *Flexible beamforming*: The deployment of PAs can transform the entire electromagnetic propagation environment, thus achieving flexible beam focusing/steering effects even with a few PAs. 3) *Scalability*: PAs can be easily activated, shifted, and released from the dielectric waveguides to accommodate various traffic demands.

Owing to the above appealing features, PASS recently becomes a focal point in both academia and industry. The first prototype of PASS has been developed by DOCOMO in 2021, and its effectiveness at 60-GHz millimeter-wave (mmWave) band has been tested [8]. The authors of [6] conceived both

X. Xu and A. Nallanathan are with the School of Electronic Engineering and Computer Science, Queen Mary University of London, London E1 4NS, U.K. (email: {x.xiaoxia, a.nallanathan}@qmul.ac.uk).

X. Mu is with the Centre for Wireless Innovation (CWI), Queen's University Belfast, Belfast, BT3 9DT, U.K. (x.mu@qub.ac.uk)

Y. Liu is with the Department of Electrical and Electronic Engineering (EEE), The University of Hong Kong, Hong Kong (e-mail: yuanwei@hku.hk).

single-waveguide architecture and multi-waveguide architecture for PASS. For multi-waveguide architecture, a single PA is activated on each waveguide, and the performance upper bound of the corresponding two-user multi-input single-output (MISO) interference channel have been derived. Furthermore, the authors of [9] considered the downlink sum rate maximization problem of a single-user PASS scenario. The locations of multiple PAs are optimized by a two-stage algorithms, where the first stage determines PAs' locations by minimizing the large-scale path loss, and the second stage refines PAs' locations to ensure constructive interference. In [10], the authors demonstrated the existence of an optimal inter-antenna spacing to maximize the array gains of PASS. Moreover, the authors of [11] considered a discrete single-waveguide PASS architecture, where the activated PAs attached at predefined locations were selected to activate by one-to-one matching.

Note that the aforementioned literatures mainly focused on either single-waveguide designs or multiple-waveguide designs where only single PA is activated at each waveguide. Up to date, how to develop a general PASS architecture for multi-user MISO communications is still less understood. The remaining open challenges are two-fold:

- The deployment of each PA impacts both the large-scale path loss and the phases of signals, which leads to the novel concept of *pinching beamforming*. Despite providing additional degree-of-freedom (DoF), efficient pinching beamforming is required to simultaneously reconfigure large-scale fading and signal phases, which is more challenging than conventional MIMO beamforming and existing flexible-antenna techniques.
- Activating multiple PAs along waveguides leads to constructive signal enhancement and destructive interference mitigation of radio waves. Hence, the cooperative deployment of PAs is crucial for multi-user communications in PASS. However, how to achieve fast cooperative deployment of multiple PAs remains to be explored, especially when the number of PAs increases.

To address above issues, this paper proposes a novel PASS-enabled downlink multi-user MISO framework. A sum rate maximization problem is formulated by jointly optimizing the newly introduced pinching beamforming and the conventional transmit beamforming. The resulting optimization problem is highly coupled and involves nonconvex complex exponential components. To tackle this problem, this paper proposes both optimization-based and learning-based methods. *First*, by reformulating the coupled optimization problem using the weighted minimum mean square error (WMMSE), we develop a majorization-minimization and penalty dual decomposition (MM-PDD) algorithm, which is guaranteed to find the stationary solution. Specifically, the Lipschitz gradient surrogate function is constructed for convex relaxation of complex exponential components. Then, the coupled optimization is decomposed by PDD theory and iteratively solved by block coordinate descent (BCD). *Secondly*, to achieve fast beamforming with a millisecond-level response, we propose a novel optimization theory-guided learning method, termed *Karush-Kuhn-Tucker (KKT)-guided dual learning (KDL)*. The key idea

is to enable machine learning (ML) to directly reconstruct Karush-Kuhn-Tucker (KKT) solutions by learning only a few dual variables in a data-driven manner. Hence, it inherits the white-box KKT solution structure, but avoids inefficient alternating block descents required by iterative optimization algorithms. We implement KDL by exploiting the powerful large language model (LLM) techniques, and comes up with a KDL-Transformer algorithm. The channel-state-information-(CSI)-to-beamforming mapping is regarded as a sequence-to-sequence learning task. By modelling both inter-PA/inter-user dependencies and CSI-beamforming dependencies, the proposed KDL-Transformer achieves stunning performance gains compared to mathematical optimization and black-box learning algorithms.

The main contributions of this work are summarized as follows.

- We propose a novel PASS-enabled downlink multi-user MISO framework, which enables the additional pinching beamforming by configuring PAs' locations. A joint transmit and pinching beamforming optimization problem is formulated to maximize the system sum rate achieved by PASS. To tackle this coupled nonconvex problem, we propose both optimization-based and learning-based methods.
- For the optimization-based method, we develop an MM-PDD algorithm. The nonconvex coupled optimization problem is first reformulated into a WMMSE problem. We derive Lipschitz gradient surrogate function based on MM to handle the nonconvex complex exponential component, and then decouple the problem based on PDD to obtain stationary solutions.
- For the learning-based method, we propose a novel KDL approach. KDL learns dual variables to reconstruct KKT solutions in a low-complexity and data-driven manner, instead of inferring all primal variables by black-box models. To unleash the potential based on LLM techniques, we develop a KDL-Transformer, which can capture both inter-PA/inter-user dependencies and CSI-beamforming dependencies to find high-quality solutions.
- We provide numerical results to demonstrate the effectiveness of the proposed framework and algorithms, which demonstrates that: 1) The proposed PASS architecture outperforms conventional hybrid beamforming architecture even only a few PAs are activated. 2) Unlike black-box learning algorithms that are stuck at inferior points, the proposed KDL-Transformer increases over 30% system performance than MM-PDD algorithm, while achieving over 7000 times faster execution on modern GPUs.

The rest of this paper is organized as follows. Section II presents the proposed PASS framework for downlink multi-user MISO communications and formulates the sum rate maximization problem. Section III develops an MM-PDD algorithm for joint digital and pinching beamforming, and Section IV proposes the KKT-guided dual learning method and develops a KDL-Transformer algorithm. Section V provides numerical results to verify the efficiency of the proposed framework and

algorithms. Finally, Section VI concludes the paper.

Notations: The variable, vector, and matrix are denoted by x , \mathbf{x} , and \mathbf{X} , respectively. $|x|$ denotes the absolute value of a real number and the modulus of a complex number. $\text{Re}\{x\}$ and $\text{Im}\{x\}$ denote the real and image parts of x , and x^H is the complex conjugate number of x . $\mathbf{1}_{N \times 1}$ denotes an N -dimension all-ones vector. \mathbf{X}^T and \mathbf{X}^H denote the transpose and the Hermitian matrix. $\|\mathbf{x}\|_\infty = \max_i |x_i|$, $\|\mathbf{x}\|$ is the vector Euclidean norm, and $\|\mathbf{X}\|$ is the matrix Frobenius norm.

II. SYSTEM MODEL AND PROBLEM FORMULATION

In this paper, we propose a PASS-enabled downlink multi-user MISO framework, as shown in Fig. 1. The BS is equipped with N waveguides and M PAs to serve K single-antenna users. Each waveguide stretches thousands of wavelengths. There are L PAs flexibly pinched along each waveguide, and the total number of PAs is $M = L \times N$. By activating PAs at different points along the waveguides, both the phases of incident signals and the large-scale fading can be altered. Let \mathcal{N} and $\mathcal{M} = \mathcal{L}_1 \cup \mathcal{L}_2 \cup \dots \cup \mathcal{L}_N$ denote the sets of all the waveguides and PAs, respectively, where $\mathcal{L}_n = \{a_{n,1}, a_{n,2}, \dots, a_{n,L}\}$ is the collection of PAs at waveguide n . To support spatial multiplexing, each waveguide is connected to a dedicated radio frequency (RF) chain, which converts the signal multiplexed at the baseband and feeds it into the waveguide. To ensure multiplexing gains, we assume $N = K$. Both waveguides and PAs are installed at a fixed height of h^{PA} , and the resulting PASS spans across a rectangular area with a size of $S_x \times S_y$ m². The three-dimension Cartesian coordinate of the feed point for the n -th waveguide is given by $\boldsymbol{\eta}_n^{\text{W}} = [0, y_n^{\text{W}}, h^{\text{PA}}]^T$, where y_n^{W} is the y -axis coordinate of this waveguide. The location of each PA $a_{n,l}$ along the n -th waveguide can be defined as $\boldsymbol{\eta}_{n,l}(x_{n,l}) = [x_{n,l}, y_{n,l}, h^{\text{PA}}]^T$, where $x_{n,l}$ is the adjustable pinched location of PA $a_{n,l}$ along x -axis, and $y_{n,l}$ is the fixed coordinate over y -axis that depends on the connected waveguide, i.e., $y_{n,l} = y_n^{\text{W}}$. Let $\mathbf{x}_n = [x_{n,1}, x_{n,2}, \dots, x_{n,L}]^T \in \mathbb{R}^{L \times 1}$ stack the x -axis locations of PAs over the n -th waveguide, which satisfy $0 \leq x_{n,1} < x_{n,2} < \dots < x_{n,L} \leq S_x, \forall n \in \mathcal{N}$. $\mathbf{X} = [\mathbf{x}_1, \mathbf{x}_2, \dots, \mathbf{x}_N] \in \mathbb{R}^{N \times L}$ stacks the locations of all PAs. Furthermore, the location of user k is denoted by $\boldsymbol{\eta}_k^{\text{U}} = [x_k^{\text{U}}, y_k^{\text{U}}, 0]^T, \forall k \in \mathcal{K}$.

A. Signal Radiation Model

Each waveguide needs to be fed with the same signal. This signal is multiplexed at the baseband through the conventional transmit beamforming \mathbf{D} , and then converted by the RF chain and fed into the waveguide for radiation. As a result, the transmitted signal of user k radiated by the PASS to the free space is given by

$$\mathbf{s}_k^{\text{TX}} = \mathbf{G}(\mathbf{X}) \mathbf{d}_k \tilde{s}_k \in \mathbb{C}^{M \times 1}, \quad (1)$$

where $\mathbf{G}(\mathbf{X}) \in \mathbb{C}^{M \times N}$ denotes the path response when the signals are propagated from the feed point of each waveguide to specific PAs, $\mathbf{d}_k \in \mathbb{C}^{N \times 1}$ denotes the conventional transmit beamforming vector for user k , and \tilde{s}_k is the data signal

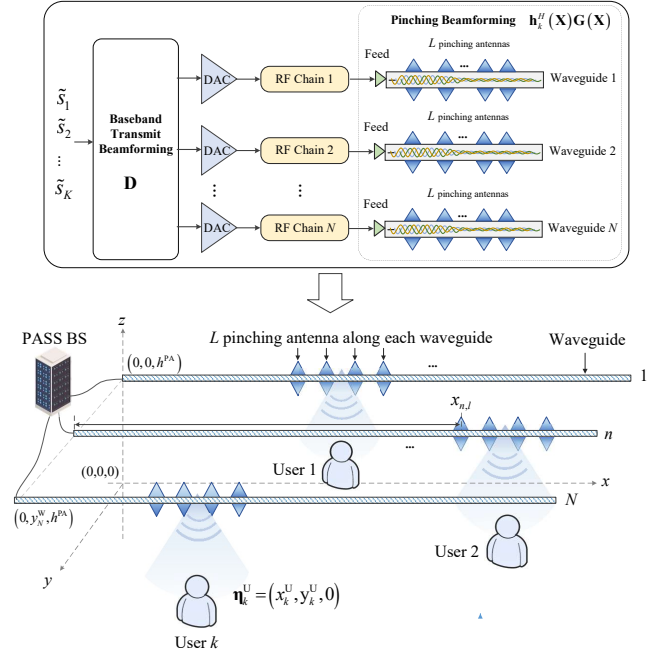


Fig. 1: PASS-enabled downlink multi-user MIMO framework, satisfying $\mathbb{E}[\tilde{s}_k^H \tilde{s}_k] = 1$. As each waveguide is connected to a subset of PAs, $\mathbf{G}(\mathbf{X})$ is a block-diagonal matrix, given by

$$\begin{aligned} \mathbf{G}(\mathbf{X}) &= \text{blkdiag}(\mathbf{g}_1(\mathbf{x}_1), \mathbf{g}_1(\mathbf{x}_2), \dots, \mathbf{g}_N(\mathbf{x}_N)) \\ &= \begin{bmatrix} \mathbf{g}_1(\mathbf{x}_1) & \mathbf{0} & \dots & \mathbf{0} \\ \mathbf{0} & \mathbf{g}_2(\mathbf{x}_2) & \dots & \mathbf{0} \\ \vdots & \vdots & \ddots & \vdots \\ \mathbf{0} & \mathbf{0} & \dots & \mathbf{g}_N(\mathbf{x}_N) \end{bmatrix}, \end{aligned} \quad (2)$$

where $\mathbf{g}_n(\mathbf{x}_n) \in \mathbb{C}^{L \times 1}$ is the response vector from the feed point of waveguide n to the associated subset of PAs in \mathcal{L}_n . The l -th element of $\mathbf{g}_n(\mathbf{x}_n)$ is given by

$$g_{n,l}(x_{n,l}) = \frac{1}{\sqrt{L}} e^{-i \frac{2\pi}{\lambda_{\text{W}}} \|\boldsymbol{\eta}_{n,l}(x_{n,l}) - \boldsymbol{\eta}_n^{\text{W}}\|} = \frac{1}{\sqrt{L}} e^{-i k n_{\text{eff}} x_{n,l}}, \quad (3)$$

where $\lambda_{\text{W}} = \frac{\lambda_f}{n_{\text{eff}}}$ is the guided wavelength, where n_{eff} denoting the effective refractive index of the dielectric waveguide [6], [14]. Moreover, $\|\boldsymbol{\eta}_{n,l}(x_{n,l}) - \boldsymbol{\eta}_n^{\text{W}}\| = x_{n,l}$ denotes the distance from waveguide n to PA $a_{n,l}$. Since the transmitting power is equally radiated by each PA along the waveguide, the amplitude of the transmitted signal is multiplied by $1/\sqrt{L}$.

We consider high-frequency bands such as millimeter-wave (mmWave) or terahertz (THz) in this work. Owing to the severe path-loss and shadowing at the high-frequency bands, the power gains of non-line-of-sight (NLoS) paths are typically negligible [12]. Hence, the channel vector can be approximated by the LoS-dominant model. Let $\mathbf{h}_{k,n}^H(\mathbf{x}_n) \in \mathbb{C}^{1 \times L}$ denote the channel vector between PAs \mathcal{L}_n and user k , which is determined by the pinching deployment \mathbf{x}_n . The l -th element of channel vector $\mathbf{h}_{k,n}^H(\mathbf{x}_n)$ indicates the channel from PA $a_{n,l}$ to user k at location $\boldsymbol{\eta}_k^{\text{U}}$, which is given by the geometric free-space spherical wavefront model [13]:

$$h_{k,n,l}^H(x_{n,l}) = \frac{\sqrt{\beta} e^{-i k r(x_{n,l}, \boldsymbol{\eta}_k^{\text{U}})}}{r(x_{n,l}, \boldsymbol{\eta}_k^{\text{U}})}, \quad (4)$$

where $\kappa = 2\pi/\lambda_f$ is the wave-domain number, and λ_f is the wavelength. The constant $\beta = c/(4\pi f_c)$ depends on the speed of light c and the carrier frequency f_c , which represents the reference channel gain at a range of unit distance (i.e., 1 meter). Moreover, $\sqrt{\beta}/r(x_{n,l}, \boldsymbol{\eta}_k^U)$ denotes the channel gain coefficient, and $r(x_{n,l}, \boldsymbol{\eta}_k^U) = \|\boldsymbol{\eta}_k^U - \boldsymbol{\eta}_{n,l}(x_{n,l})\|$ is the distance between PA $a_{n,l}$ and user k , which is computed by

$$r(x_{n,l}, \boldsymbol{\eta}_k^U) = \sqrt{(x_{n,l} - x_k^U)^2 + (y_{n,l}^{\text{PA}} - y_k^U)^2 + (h^{\text{PA}})^2}. \quad (5)$$

Let $\mathbf{h}_k^H(\mathbf{X}) = [\mathbf{h}_{k,1}^H(\mathbf{x}_1), \mathbf{h}_{k,2}^H(\mathbf{x}_2), \dots, \mathbf{h}_{k,N}^H(\mathbf{x}_N)] \in \mathbb{C}^{1 \times M}$ stack the channel vectors from all the PAs to user k . Hence, the received signal at user k through the channels manipulated by PAs can be compactly expressed by

$$y_k = \underbrace{\mathbf{h}_k^H(\mathbf{X}) \mathbf{G}(\mathbf{X}) \mathbf{d}_k \tilde{s}_k}_{\text{desired signal}} + \underbrace{\sum_{k' \neq k} \mathbf{h}_k^H(\mathbf{X}) \mathbf{G}(\mathbf{X}) \mathbf{d}_{k'} \tilde{s}_{k'} + n_k}_{\text{multi-user interference}}. \quad (6)$$

The effective gains of user k can be given by

$$E_k = \frac{\beta}{L} \left| \sum_{n \in \mathcal{N}} \sum_{l \in \mathcal{L}_n} \frac{e^{-i\kappa(r(x_{n,l}, \boldsymbol{\eta}_k^U) + n_{\text{eff}} x_{n,l})}}{r(x_{n,l}, \boldsymbol{\eta}_k^U)} d_{n,k} \right|^2. \quad (7)$$

Furthermore, the interference experienced by user k caused by the transmitted signal of user k' can be represented by

$$I_{k,k'} = \frac{\beta}{L} \left| \sum_{n \in \mathcal{N}} \sum_{l \in \mathcal{L}_n} \frac{e^{-i\kappa(r(x_{n,l}, \boldsymbol{\eta}_k^U) + n_{\text{eff}} x_{n,l})}}{r(x_{n,l}, \boldsymbol{\eta}_k^U)} d_{n,k'} \right|^2. \quad (8)$$

Therefore, the signal-to-interference-and-noise ratio (SINR) of user m is given by

$$\gamma_k = \frac{|\mathbf{h}_k^H(\mathbf{X}) \mathbf{G}(\mathbf{X}) \mathbf{d}_k|^2}{\sum_{k' \neq k} |\mathbf{h}_k^H(\mathbf{X}) \mathbf{G}(\mathbf{X}) \mathbf{d}_{k'}|^2 + \sigma^2} = \frac{E_k}{\sum_{k' \neq k} I_{k,k'} + \sigma^2}. \quad (9)$$

To enhance SINR of users, the transmit beamforming and the pinching beamforming should be jointly designed to achieve constructive interference of radio waves for improving effective gains E_k in (7), while achieving destructive interference for mitigating multi-user interference $I_{k,k'}$ in (8).

B. Problem Formulation and Conversion

The key objective of this paper is to maximize the sum rate of users in PASS by jointly optimizing the transmit beamforming and the pinching beamforming. This is formulated as the following sum rate maximization problem:

$$(P0) \max_{\mathbf{X}, \mathbf{D}} \sum_{k \in \mathcal{K}} \log_2 \left(1 + \frac{|\mathbf{h}_k^H(\mathbf{X}) \mathbf{G}(\mathbf{X}) \mathbf{d}_k|^2}{\sum_{k' \neq k} |\mathbf{h}_k^H(\mathbf{X}) \mathbf{G}(\mathbf{X}) \mathbf{d}_{k'}|^2 + \sigma^2} \right) \quad (10a)$$

$$\text{s.t. (C1): } x_{n,l} - x_{n,l-1} \geq \Delta_{\min}, \forall 1 < l \leq L, \forall n \in \mathcal{N}, \quad (10b)$$

$$(C2): 0 \leq x_{n,l} \leq S_x, \forall l \in \mathcal{M}, \quad (10c)$$

$$(C3): \sum_{k \in \mathcal{K}} \|\mathbf{d}_k\|_2^2 \leq P, \quad (10d)$$

where (C1) ensures the minimum antenna space Δ_{\min} to avoid mutual coupling, (C2) guarantees the location of each PA does not exceed the maximum length of the connected waveguide, and (C3) denotes the maximum transmitting power of the BS. It is worth noting that (P0) is a highly non-convex optimization problem with strongly coupled variables. Conventionally, we can solve (P0) by decomposing it into decoupled problems and invoking convex approximation techniques to find suboptimal solutions. In the remaining sections, we will first come up with an MM-PDD algorithm based on conventional optimization theory to achieve stationary solution of (P0). Then, by revisiting the KKT solution structure of the beamforming problem, a novel learning algorithm will be developed to further deal with the coupled transmit and pinching beamforming optimization.

III. OPTIMIZATION BASED JOINT TRANSMIT AND PINCHING BEAMFORMING

To solve problem (P0), we first reformulate the SINR expression into a more tractable form based on WMMSE. Then, an MM-PDD optimization algorithm is developed, which recasts the coupling constraints into the augmented Lagrangian function, thus alternatively updating multi-block variables in a BCD style. During the block variable update, the nonconvex component is relaxed by majorization minimization, where the Lipschitz gradient surrogate is employed as the block surrogate for stable convergence.

A. WMMSE-based Reformulation

Assume \tilde{s}_k and n_k are independent. Therefore, the mean square error (MSE) of user k can be given by [15]

$$e_k(\mathbf{X}, \mathbf{D}, \mathbf{v}) \triangleq \mathbb{E} [|\hat{y}_k - \tilde{s}_k|^2] = \mathbb{E} [(v_k y_k - \tilde{s}_k)^H (v_k y_k - \tilde{s}_k)] = \sum_{i \in \mathcal{K}} |v_i \mathbf{h}_i^H(\mathbf{X}) \mathbf{G}(\mathbf{X}) \mathbf{d}_i|^2 + \sigma^2 |v_k|^2 + 1 - 2 \text{Re} \{ v_k \mathbf{h}_k^H(\mathbf{X}) \mathbf{G}(\mathbf{X}) \mathbf{d}_k \}, \quad (11)$$

where $\hat{y}_k = v_k y_k$ is the estimated signal received by user k and v_k denotes the channel equalizer.

Lemma 1: The optimal solution of the constrained sum rate maximization problem (P1) is equivalent to the following WMMSE problem:

$$(P1) \min_{\mathbf{X}, \mathbf{D}, \mathbf{v}, \boldsymbol{\alpha}} \sum_{k=1}^K (\alpha_k e_k(\mathbf{X}, \mathbf{D}, v_k) - \log_2 \alpha_k), \quad (12a)$$

$$\text{s.t. (C1) - (C3),} \quad (12b)$$

where α_k denotes the weighting factor. By fixing other variables, the optimal solution of α_k and v_k can be given by

$$v_k^{\text{opt}} = J_k^{-1} \mathbf{d}_k^H \mathbf{G}_k^H(\mathbf{X}) \mathbf{h}_k(\mathbf{X}), \forall k \in \mathcal{K}, \quad (13)$$

$$\alpha_k^{\text{opt}} = (1 - \mathbf{d}_k^H \mathbf{G}^H(\mathbf{X}) \mathbf{h}_k(\mathbf{X}) J_k^{-1} \mathbf{h}_k^H(\mathbf{X}) \mathbf{G}(\mathbf{X}) \mathbf{d}_k)^{-1}, \quad (14)$$

where $J_k \triangleq \sum_{i \in \mathcal{K}} \mathbf{h}_i^H(\mathbf{X}) \mathbf{G}(\mathbf{X}) \mathbf{d}_i \mathbf{d}_i^H \mathbf{G}^H(\mathbf{X}) \mathbf{h}_i(\mathbf{X}) + \sigma^2$ denotes the covariance of signal y_k received by user k .

Proof. See Appendix A. \square

The above WMMSE-based reformulation converts the fractional SINR into a more tractable form. We could follow the BCD method to optimize (P1) if it is multi-convex with respect to (w.r.t.) each block variable \mathbf{D} and \mathbf{x} . However, the complex exponential components and the reciprocals of distances in (11) render the non-convexity of (P1) w.r.t. \mathbf{x} , which is strongly coupled with \mathbf{D} . To solve this nonconvex coupled problem, we invoke the PDD theory with a majorization minimization procedure, thus ensuring the stable convergence to a critical point.

B. The Proposed MM-PDD Algorithm

We first transform (P1) into a more tractable augmented Lagrangian (AL) problem, and then establish Lipschitz gradient surrogate for convex relaxation based on the MM method. To this end, we newly introduce auxiliary variable $s_{k,n,l} = r(x_{n,l}, \boldsymbol{\eta}_k^U) = \sqrt{(x_{n,l} - x_k^U)^2 + \psi_{k,n,l}^2}$ to represent the PA-user distances, $\theta_{k,n,l} = \kappa(s_{k,n,l} + n_{\text{eff}}x_{n,l})$ to indicate the PASS-modified phase of user k 's signal, and $u_{k,n,l} = \sqrt{\beta}/\sqrt{L}e^{-i\theta_{k,n,l}}/r(x_{n,l}, \boldsymbol{\eta}_k^U)$ to signify the equivalent pinching beamforming coefficient of user k 's signal radiated by PA $a_{n,l}$. This leads to the following equality constraints:

$$b_{k,n,l}^u \triangleq u_{k,n,l} \sqrt{(x_{n,l} - x_k^U)^2 + \psi_{k,n,l}^2} - \phi e^{-i\theta_{k,n,l}} = 0, \quad (15a)$$

$$b_{k,n,l}^\theta \triangleq \theta_{k,n,l} - \kappa(s_{k,n,l} + n_{\text{eff}}x_{n,l}) = 0, \quad (15b)$$

$$b_{k,n,l}^s \triangleq \sqrt{(x_{n,l} - x_k^U)^2 + \psi_{k,n,l}^2} - s_{k,n,l} = 0, \quad (15c)$$

where $\phi \triangleq \sqrt{\beta}/\sqrt{L}$ is a constant, and $\psi_{k,n,l} = \sqrt{(y_{n,l}^{\text{PA}} - y_k^u)^2 + (h^{\text{PA}})^2}$ is fixed for each channel realization. Moreover, we define $q_{k,k'} = \mathbf{h}_k^H(\mathbf{X}) \mathbf{G}(\mathbf{X}) \mathbf{d}_{k'}$ as the path response of user k to receive the signal of user k' . From the above definitions, $q_{k,k'}$ satisfies the equality constraint:

$$b_{k,k'}^q \triangleq q_{k,k'} - \mathbf{u}_k^T \boldsymbol{\Sigma} \mathbf{d}_{k'} = 0, \quad \forall k, k' \in \mathcal{K}, \quad (16)$$

where $\mathbf{u}_k^T = [\mathbf{u}_{k,1}^T, \mathbf{u}_{k,2}^T, \dots, \mathbf{u}_{k,N}^T] \in \mathbb{C}^{1 \times M}$ stacks the pinching beamforming coefficients for all the PAs, and $\mathbf{u}_{k,n}^T = [u_{k,n,1}, u_{k,n,2}, \dots, u_{k,n,L}]^T \in \mathbb{C}^{1 \times L}$ is the pinching beamforming vector of user k using PAs in subset \mathcal{L}_n . Moreover, $\boldsymbol{\Sigma} = \text{blkdiag}(\mathbf{1}_{L \times 1}, \mathbf{1}_{L \times 1}, \dots, \mathbf{1}_{L \times 1}) \in \mathbb{R}^{M \times N}$ is a block diagonal matrix.

By penalizing and dualizing equalities into the objective function, the AL function of (P1) can be constructed by:

$$(P2) \quad \min_{\mathbf{x}, \mathbf{D}, \boldsymbol{\alpha}, \mathbf{v}, \mathbf{S}, \mathbf{U}, \boldsymbol{\theta}, \mathbf{Q}} \sum_{k=1}^K (\alpha_k e_k(\mathbf{Q}, v_k^{\text{opt}}) - \log_2 \alpha_k) + \frac{1}{2\rho} \times \sum_{k \in \mathcal{K}} \left(\|\mathbf{B}_k^u + \rho \boldsymbol{\lambda}_k^u\|^2 + \|\mathbf{B}_k^\theta + \rho \boldsymbol{\lambda}_k^\theta\|^2 + \|\mathbf{B}_k^s + \rho \boldsymbol{\lambda}_k^s\|^2 + \|\mathbf{b}_k^q + \rho \boldsymbol{\lambda}_k^q\|^2 \right),$$

s.t. (C1) - (C3),

where $\mathbf{Q} = \{q_{k,k'}\} \in \mathbb{C}^{K \times K}$ and $\mathbf{U} = [\mathbf{u}_1, \mathbf{u}_2, \dots, \mathbf{u}_K] \in \mathbb{R}^{M \times K}$. $\mathbf{B}_k^u = \{b_{k,n,l}^u\}$, $\mathbf{B}_k^\theta = \{b_{k,n,l}^\theta\}$, and $\mathbf{B}_k^s = \{b_{k,n,l}^s\}$

stack the residuals of the equality constraints in (15), and $\mathbf{b}_k^q = \{b_{k',k}^q\}$ stacks the residual of equality constraint (16). Moreover, $\boldsymbol{\lambda}_k^u \in \mathbb{C}^{N \times L}$, $\boldsymbol{\lambda}_k^\theta \in \mathbb{C}^{N \times L}$, $\boldsymbol{\lambda}_k^s \in \mathbb{R}^{N \times L}$, and $\boldsymbol{\lambda}_k^q \in \mathbb{C}^{K \times 1}$ are dual variables corresponding to (15) and (16), respectively. By fixing v_k^{opt} , the MSE is rewritten as a convex function of w.r.t. $q_{k,k'}$:

$$e_k(\mathbf{Q}, v_k^{\text{opt}}) = |v_k^{\text{opt}}|^2 \left(\sum_{k' \in \mathcal{K}} |q_{k,k'}|^2 + \sigma^2 \right) + 1 - 2\text{Re}\{v_k^{\text{opt}} q_{k,k}\}. \quad (17)$$

Now, the nonconvexity of problem (P2) only lies in the AL term $\frac{1}{2\rho} \|\mathbf{B}_k^u + \rho \boldsymbol{\lambda}_k^u\|^2 + \frac{1}{2\rho} \|\mathbf{B}_k^s + \rho \boldsymbol{\lambda}_k^s\|^2$ w.r.t. \mathbf{x} and $\boldsymbol{\theta}$, which is the sum of terms

$$L_{k,n,l}^{\text{NC}} = \frac{1}{2\rho} \left(u_{k,n,l} \sqrt{(x_{n,l} - x_k^U)^2 + \psi_{k,n,l}^2} - \phi e^{-i\theta_{k,n,l}} + \rho \lambda_{k,n,l}^u \right)^2 + \frac{1}{2\rho} \left(\sqrt{(x_{n,l} - x_k^U)^2 + \psi_{k,n,l}^2} - s_{k,n,l} + \rho \lambda_{k,n,l}^s \right)^2. \quad (18)$$

We construct convex surrogate functions over the block variables \mathbf{x} and $\boldsymbol{\theta}$ during the block update of PDD, respectively.

On the one hand, $L_{k,n,l}^{\text{NC}}$ is a difference of convex (D.C.) function w.r.t. $x_{n,l}$. The D.C. function $L_{k,n,l}^{\text{DC}}(x_{n,l})$ is defined in (19a), as shown in the bottom of the next page, where $\Omega_{k,n,l} \triangleq \text{Re}\{u_{k,n,l}^H (\lambda_{k,n,l}^u - \frac{\phi e^{-i\theta_{k,n,l}}}{\rho})\} + (\lambda_{k,n,l}^s - \frac{s_{k,n,l}}{\rho})$ is the coefficient of the convex function $\sqrt{(x_{n,l} - x_k^U)^2 + \psi_{k,n,l}^2}$. When $\Omega_{k,n,l}$ is a negative coefficient, function $L_{k,n,l}^{\text{DC}}(x_{n,l})$ contains a concave component $L^{\text{CC}}(x_{n,l}) = \Omega_{k,n,l} \sqrt{(x_{n,l} - x_k^U)^2 + \psi_{k,n,l}^2}$. We handle the D.C. component using the concave-convex procedure (CCCP), which is a special case of MM for D.C. programming [16], [17]. CCCP utilizes the first-order Taylor expansion of $L^{\text{CC}}(x_{n,l})$ as its tight upper bound, as presented in (19) in the bottom of this page, where the derivative $\nabla_x L_{k,n,l}^{\text{CC}}(x_{n,l}^{(t-1)})$ can be given by

$$\nabla_{x_{n,l}} L_{k,n,l}^{\text{CC}}(x_{n,l}^{(t-1)}) = \frac{\Omega_{k,n,l} (x_{n,l}^{(t-1)} - x_k^U)}{(x_{n,l}^{(t-1)} - x_k^U)^2 + \psi_{k,n,l}^2}. \quad (20)$$

On the other hand, $L_{k,n,l}^{\text{NC}}$ involves the complex exponential component $L^{\text{EXP}}(\theta_{k,n,l}) = -\phi \text{Re}\{(\lambda_{k,n,l}^u + \frac{u_{k,n,l} s_{k,n,l}}{\rho}) e^{i\theta_{k,n,l}}\}$, which periodically switch between convex and concave functions over the feasible range of $\theta_{k,n,l} \in \mathbb{R}$. To convert this intractable nonconvex component, we construct Lipschitz gradient surrogate based on the MM method [18], which can be defined as follows.

Definition 1 (Lipschitz gradient surrogate). The Lipschitz gradient surrogate of a function $f(\boldsymbol{\theta})$ is defined as

$$\mathcal{S}(\boldsymbol{\theta}, \boldsymbol{\theta}^{(t-1)}) = f(\boldsymbol{\theta}^{(t-1)}) + \left(\nabla_{\boldsymbol{\theta}} f(\boldsymbol{\theta}^{(t-1)}) \right)^T (\boldsymbol{\theta} - \boldsymbol{\theta}^{(t-1)}) + \frac{\rho}{2} \|\boldsymbol{\theta} - \boldsymbol{\theta}^{(t-1)}\|^2, \quad (21)$$

where ρ is the Lipschitz gradient constant that ensures $\|\nabla_{\boldsymbol{\theta}} f(\boldsymbol{\theta}_1) - \nabla_{\boldsymbol{\theta}} f(\boldsymbol{\theta}_2)\| \leq \rho \|\boldsymbol{\theta}_1 - \boldsymbol{\theta}_2\|$, $\forall \boldsymbol{\theta}_1, \boldsymbol{\theta}_2$.

The Lipschitz gradient surrogate $\mathcal{S}(\boldsymbol{\theta}, \boldsymbol{\theta}^{(t-1)})$ establishes an MM upper bound of $f(\boldsymbol{\theta})$ when the gradient $\nabla_{\boldsymbol{\theta}} f(\boldsymbol{\theta}^{(t-1)})$ is ϱ -Lipschitz continuous [17], [18]. Compared to the first-order Taylor expansion, Lipschitz gradient surrogate exploits an extra second-order regularization term, which achieves a strict convexity approximation and thus improves the convergence guarantees. To apply MM, we introduce the following lemma to construct Lipschitz gradient surrogate of the exponential term $L^{\text{EXP}}(\theta_{k,n,l}) = -\phi \text{Re} \left\{ \left(\lambda_{k,n,l}^u + \frac{u_{k,n,l} s_{k,n,l}}{\rho} \right) e^{i\theta_{k,n,l}} \right\}$.

Lemma 2: Given $a, \theta \in \mathbb{R}$ and $c \in \mathbb{C}$, function $-\text{Re} \{ c e^{i(a\theta)} \}$ has Lipschitz-continuous gradient w.r.t. θ , and the Lipschitz constant is given by $\varrho^\theta = a^2 |c|$.

Proof. See Appendix B. \square

From the above Lemma, the Lipschitz gradient surrogate of $L_{k,n,l}^{\text{EXP}}(\theta_{k,n,l})$ can be constructed by (22), which is defined in the bottom of this page. Furthermore, the corresponding Lipschitz constant can be given by

$$\varrho_{k,n,l}^\theta = \phi \left| \lambda_{k,n,l}^u + \frac{u_{k,n,l} s_{k,n,l}}{\rho} \right|. \quad (23)$$

Based on the PDD method [19], we can now solve (P1) by alternatively optimizing the following four subproblems in a BCD manner in the inner loop, while updating the dual variables and penalty factor in the outer loop.

(i) *Subproblem w.r.t. $\{\mathbf{D}, \mathbf{Q}\}$:* The transmit beamforming \mathbf{D} and the path response \mathbf{Q} are jointly optimized by solving the following constrained optimization problem:

$$\min_{\mathbf{Q}, \mathbf{D}} \sum_{k=1}^K \alpha_k e_k(\mathbf{Q}, v_k^{\text{opt}}) + \frac{1}{2\rho} \|\mathbf{Q} - \mathbf{U}^T \boldsymbol{\Sigma} \mathbf{D} + \rho \boldsymbol{\lambda}^q\|^2, \quad (24a)$$

$$\text{s.t. (C3).} \quad (24b)$$

The optimal solution of $q_{k,k'}$ can be obtained by

$$q_{k,k'}^* = \frac{2v_k \delta_{k,k'} - \lambda_{k,k'}^q + \frac{1}{\rho} \mathbf{u}_k^T \boldsymbol{\Sigma} \mathbf{d}_k}{2|v_k|^2 + \frac{1}{\rho}}, \quad \forall k, k' \in \mathcal{K}, \quad (25)$$

where $\delta_{k,k'} = 1$ if $k = k'$ and $\delta_{k,k'} = 0$ otherwise.

(ii) *Subproblem w.r.t. \mathbf{X} :* Combining the convex components and the block surrogate function, the pinching deployment \mathbf{X} can be updated by solving

$$\min_{\mathbf{X}} \frac{1}{2\rho} \sum_{k \in \mathcal{K}} \|\boldsymbol{\theta}_k - \kappa(\mathbf{s}_k + n_{\text{eff}} \mathbf{X})\|^2 + \sum_{k \in \mathcal{K}} \sum_{n \in \mathcal{N}} \sum_{l \in \mathcal{L}_n} \widehat{L}_{k,n,l}^{\text{DC}}(x_{n,l})$$

$$L_{k,n,l}^{\text{DC}}(x_{n,l}) = \frac{1}{2\rho} (u_{k,n,l}^2 + 1) (x_{n,l} - x_k^{\text{U}})^2 + \Omega_{k,n,l} \sqrt{(x_{n,l} - x_k^{\text{U}})^2 + \psi_{k,n,l}^2}, \quad (\text{if } \Omega_{k,n,l} < 0), \quad (19a)$$

$$\leq \widehat{L}_{k,n,l}^{\text{DC}}(x_{n,l}) = \frac{1}{2\rho} (u_{k,n,l}^2 + 1) (x_{n,l} - x_k^{\text{U}})^2 + \nabla_{x_{n,l}} L_{k,n,l}^{\text{CC}}(x_{n,l}^{(t-1)}) (x_{n,l} - x_{n,l}^{(t-1)}), \quad (\text{if } \Omega_{k,n,l} < 0). \quad (19b)$$

$$L_{k,n,l}^{\text{EXP}}(\theta_{k,n,l}) \leq \widehat{L}_{k,n,l}^{\text{EXP}}(\theta_{k,n,l}) = L_{k,n,l}^{\text{EXP}}(\theta_{k,n,l}^{(t-1)}) + \nabla_{\theta} L_{k,n,l}^{\text{EXP}}(\theta_{k,n,l}^{(t-1)}) (\theta_{k,n,l} - \theta_{k,n,l}^{(t-1)}) + \left| \frac{\varrho_{k,n,l}^\theta}{2} (\theta_{k,n,l} - \theta_{k,n,l}^{(t-1)}) \right|^2, \quad (22a)$$

$$\nabla_{\theta} L_{k,n,l}^{\text{EXP}}(\theta) = \phi \text{Re} \left\{ \lambda_{k,n,l}^u + \frac{u_{k,n,l} s_{k,n,l}}{\rho} \right\} \sin \theta + \phi \text{Im} \left\{ \lambda_{k,n,l}^u + \frac{u_{k,n,l} s_{k,n,l}}{\rho} \right\} \cos \theta. \quad (22b)$$

Algorithm 1 MM-PDD algorithm Using Lipschitz gradient surrogate

Input: Users' locations $\boldsymbol{\eta}^{\text{U}}$ and feed points' locations $\boldsymbol{\eta}^{\text{W}}$.

- 1: Initialize primal variables \mathbf{x} , \mathbf{D} , \mathbf{Q} , and \mathbf{U} .
- 2: Initialize dual variables $\boldsymbol{\lambda}^{(0)} = \mathbf{0}$ and tolerance threshold.
- 3: **for** $t = 1, 2, \dots, T_{\text{max}}$ **do**
*/** MM-BCD procedure:*
- 4: **while** convergence criterion is not satisfied **do**
- 5: Update v_k and α_k by (13) and (14), $\forall k \in \mathcal{K}$.
- 6: Update $\{\mathbf{D}, \mathbf{Q}\}$ by solving (24) while fixing remaining variables.
- 7: Update \mathbf{x} by solving (26) while fixing remaining variables, and then update \mathbf{U} by (28).
- 8: Update $\{\boldsymbol{\theta}, \mathbf{S}\}$ by (30) using Lipschitz gradient surrogate (22a).
- 9: **end while**
- 10: **if** $\|\mathbf{B}^{(t)}\|_{\infty} \leq 0.9 \|\mathbf{B}^{(t-1)}\|_{\infty}$ **then**
- 11: Update dual variables $\boldsymbol{\lambda}^{(t+1)} \leftarrow \boldsymbol{\lambda}^{(t)} + \frac{1}{\rho^{(t)}} \mathbf{B}^{(t)}$.
- 12: **else**
- 13: Update penalty parameter $\rho^{(t+1)} \leftarrow \rho^{(t)} \cdot 0.85$.
- 14: **end if**
- 15: Algorithm terminates if $\|\mathbf{B}^{(t)}\|_{\infty} \leq \epsilon$.
- 16: **end for**

Output: \mathbf{X}, \mathbf{D} .

$$\text{s.t. (C1), (C2).} \quad (26)$$

The optimal solution of this convex quadratic programming problem can be solved by the interior point method [20].

(iii) *Subproblem w.r.t. \mathbf{U} :* The effective pinching beamforming coefficients \mathbf{U} can be obtained by solving the unconstrained convex quadratic optimization problem:

$$\min_{\mathbf{U}} \sum_{k \in \mathcal{K}} \left(\|\mathbf{R}_k \mathbf{u}_k + \boldsymbol{\zeta}_k\|^2 + \|\mathbf{q}_k + \rho \boldsymbol{\lambda}_k^q - \mathbf{u}_k^T \boldsymbol{\Sigma} \mathbf{D}\|^2 \right), \quad (27)$$

where $\mathbf{R}_k = \text{diag}(r_{k,1,1}, r_{k,1,2}, \dots, r_{k,N,L}) \in \mathbb{R}^{M \times M}$, and $r_{k,n,l} = r(x_{n,l}, \boldsymbol{\eta}_k^{\text{U}})$. Moreover, $\boldsymbol{\zeta}_{k,n,l} = \rho \lambda_{k,n,l}^u - \phi e^{-i\theta_{k,n,l}}$, and vector $\boldsymbol{\zeta}_k = [\zeta_{k,1,1}, \zeta_{k,1,2}, \dots, \zeta_{k,N,L}]^T \in \mathbb{C}^{M \times 1}$. Hence, the closed-form solution of \mathbf{u}_k , $\forall k \in \mathcal{K}$, can be derived as

$$\mathbf{u}_k^* = (\mathbf{R}_k^H \mathbf{R}_k + \boldsymbol{\Sigma} \mathbf{D} \mathbf{D}^H \boldsymbol{\Sigma}^H)^{-1} (\boldsymbol{\Sigma} \mathbf{D} (\mathbf{q}_k + \rho \boldsymbol{\lambda}_k^q)^H - \mathbf{R}_k^H \boldsymbol{\zeta}_k). \quad (28)$$

(iv) *Subproblem w.r.t. $\{\theta, \mathbf{S}\}$* : The signal phases θ and the PA-user distance \mathbf{S} can be updated by solving the unconstrained convex optimization problem:

$$\begin{aligned} \min_{\theta, \mathbf{S}} \sum_{n,l} \sum_k & \left[\frac{1}{2\rho} (\theta_{k,n,l} - \kappa(s_{k,n,l} + n_{\text{eff}} x_{n,l}) + \rho \lambda_{k,n,l}^\theta)^2 \right. \\ & + \nabla_{\theta_{k,n,l}} L_{k,n,l}^{\text{EXP}}(\theta_{k,n,l}^{(t-1)}) \theta_{k,n,l} + \frac{\varrho_{k,n,l}^\theta}{2} (\theta_{k,n,l} - \theta_{k,n,l}^{(t-1)})^2 \\ & \left. + \frac{1}{2\rho} \left(\sqrt{(x_{n,l} - x_k^{\text{U}})^2 + \psi_{k,n,l}^2} - s_{k,n,l} + \rho \lambda_{k,n,l}^{\text{S}} \right)^2 \right], \quad (29) \end{aligned}$$

where the optimal solution can be given by

$$\begin{aligned} \theta_{k,n,l}^* &= \frac{\varrho_{k,n,l}^\theta \theta_{k,n,l}^{(t-1)} - \lambda_{k,n,l}^\theta + \frac{\kappa}{\rho} (s_{k,n,l} + n_{\text{eff}} x_{n,l}) - \nabla_{\theta} L^{\text{EXP}}(\theta_{k,n,l}^{(t-1)})}{\varrho_{k,n,l}^\theta + \frac{1}{\rho}}, \\ s_{k,n,l}^* &= \frac{r(x_{n,l}, \boldsymbol{\eta}_k^{\text{U}}) + \rho \lambda_{k,n,l}^{\text{S}} + \kappa (\theta_{k,n,l} + \rho \lambda_{k,n,l}^\theta - \kappa n_{\text{eff}} x_{n,l})}{1 + \kappa^2}. \quad (30) \end{aligned}$$

Algorithm 1 summarizes the iterative procedure of MM-PDD. By alternatively optimizing the coupled variables and address the nonconvex components using the CCCP and Lipschitz gradient surrogate, the objective value (i.e., the AL function) will be non-increasing through each BCD update in the inner loop [16], [17]. Therefore, MM-PDD is guaranteed to converge to a stationary point according to the analysis in [19]. However, obtaining a high quality solution $\{\mathbf{X}^*, \mathbf{D}^*\}$ in this way is very time consuming, and is prone to getting stuck in local optimums, which motivates us to further develop the learning-based approach.

IV. LEARNING-BASED JOINT TRANSMIT AND PINCHING BEAMFORMING

In this section, we introduce preliminaries on learning-based methods and present the fundamentals of the proposed KDL. Then, a KDL-Transformer is further developed for joint transmit and pinching beamforming.

A. Preliminaries on Learning to Optimize

The non-convex coupled sum rate optimization can be written in the following form:

$$\begin{aligned} (\mathcal{P}_{\mathbf{z}}) \min_{\mathbf{X}, \mathbf{D}} & F_0(\mathbf{X}, \mathbf{D}; \mathbf{z}), \quad (31a) \\ \text{s.t. } & f_i(\mathbf{X}) \leq 0, \forall i \in \mathcal{F}_x, \quad f_j(\mathbf{D}) \leq 0, \forall j \in \mathcal{F}_D. \quad (31b) \end{aligned}$$

where \mathbf{z} is the system parameter vector (e.g., CSI), and \mathbf{X} and \mathbf{D} denote the optimization variable blocks, which are coupled in the objective function $F_0(\mathbf{X}, \mathbf{D}; \mathbf{z})$. Moreover, \mathcal{F}_x and \mathcal{F}_D denote the sets of F_x and F_D inequality constraints, respectively. All the functions in (31) are differentiable and smooth, but may be nonlinear and non-convex.

Generally, the optimization-based algorithm alternatively optimizes the coupled variables in $\mathcal{P}_{\mathbf{z}}$ through an iterative process and relies on convex surrogate. To overcome their shortcomings, the concept of learning to optimize (L2O) has emerged [21], which trains ML model parameters \mathbf{w} to learn

the mapping from input parameters \mathbf{z} to desired solutions $\widehat{\mathbf{X}}$, i.e., $\widehat{\mathbf{X}} \triangleq \widehat{\mathbf{X}}_{\mathbf{w}}(\mathbf{z})$. Thus, optimization variables can be simultaneously predicted without requiring sophisticated alternating computations or iterative procedures. Despite the attractive promises of L2O, how to efficiently deal with nonconvex coupled optimization and to achieve comparative performance with conventional optimization method are still open challenges. For this purpose, existing L2O methods can be roughly classified into two categories, i.e., end-to-end learning and unfolding-based learning.

1) *End-to-end learning*: L2O can train the learning model parameters \mathbf{w} in an end-to-end fashion, which directly takes the observed system parameters \mathbf{z} as the input of ML model, and then predicts solutions \mathbf{X} and \mathbf{D} . As ML model (e.g., deep neural networks) can approximate arbitrary nonconvex functions, the end-to-end learning can mimic high-quality solution structure based on supervised learning. The model parameters \mathbf{w} are trained to minimize the mean-square-error (MSE) loss function:

$$\min_{\mathbf{w}} \left\| \mathbf{X}^* - \widehat{\mathbf{X}}_{\mathbf{w}}(\mathbf{z}) \right\|^2 + \left\| \mathbf{D}^* - \widehat{\mathbf{D}}_{\mathbf{w}}(\mathbf{z}) \right\|^2, \quad (32)$$

where $\widehat{\mathbf{X}}_{\mathbf{w}}(\mathbf{z})$ and $\widehat{\mathbf{D}}_{\mathbf{w}}(\mathbf{z})$ denote the solution predicted by ML model parameters \mathbf{w} for the given input parameters \mathbf{z} . However, supervised learning requires a large-scale dataset of pre-solved instances (samples), which is impractical for a nonconvex coupled optimization problem, especially when the system complexity (e.g., number of users/antennas) increases. Therefore, the unsupervised learning has become a viable option, which trains the model parameters \mathbf{w} by employing the optimization objective as the loss function:

$$\mathbf{w} = \arg \min_{\mathbf{w}} F_0 \left(\widehat{\mathbf{X}}_{\mathbf{w}}(\mathbf{z}), \widehat{\mathbf{D}}_{\mathbf{w}}(\mathbf{z}) \right). \quad (33)$$

However, as unsupervised learning relies on gradient descent, it is also prone to saddle points and local minimums when tackle coupled and non-convex optimization problem.

2) *Deep unfolding-based optimization*: To guide the ML model training through the optimization theory and to seek theoretical guarantees, deep unfolding further proposes to unrolls an iterative optimization algorithm by a sequence of neural network (NN) layers [22], [23], e.g., unfolding WMMSE for transmit beamforming optimization. The NN layers are trained to mimic the iterative computation procedure of conventional algorithms. However, performing such unrolling procedure requires closed-form solutions to be fully understood for coupled optimization problem. Furthermore, the design principle of deep unfolding inherits the iterative update nature of conventional optimization algorithm, which may still limit its computational efficiency in practical applications.

B. The Proposed KKT-guided Dual Learning Approach

To overcome the aforementioned challenges, we propose a novel theory-guided end-to-end learning architecture in this paper, namely KDL, which can efficiently tackle the coupled beamforming optimization problem. Unlike previous end-to-end learning or unfolding-based learning, KDL directly trains ML models to approximate the KKT solution structure of some

block optimization variables, whose explicit KKT-conditioned solution structure is easy to be derived by Lagrangian duality method. KDL learns dual variables that are required to reconstruct KKT solutions of these block optimization variables. The dual variables can be jointly inferred with the remaining optimization variables that lack closed-form KKT solution structure using the end-to-end unsupervised learning. Therefore, KDL can capitalize on the white-box solution structure obtained from the optimization theory, while inheriting the efficient execution nature of the data-driven method for high-quality solution exploration.

1) *Fundamentals of KDL*: To illustrate the fundamental principles of KDL, we consider that block variables \mathbf{D} possess explicit KKT solutions, while the closed-form solutions of remaining block variables \mathbf{X} are difficult to obtain. By fixing block variables \mathbf{X} , the Lagrangian function w.r.t. block variable \mathbf{D} is given by

$$L_{\text{Dual}}(\mathbf{D}, \boldsymbol{\lambda}; \mathbf{X}, \mathbf{z}) = F_0(\mathbf{D}; \mathbf{X}, \mathbf{z}) + \sum_{j \in \mathcal{F}_D} \lambda_j f_j(\mathbf{D}, \boldsymbol{\lambda}), \quad (34)$$

where $\boldsymbol{\lambda} \in \mathbb{R}^{F_D \times 1}$ denotes the dual variables for all inequality constraints in (31b). The KKT conditions corresponding to problem (\mathcal{P}_z) can be expressed as [24]

$$\begin{cases} \text{(i)} f_j(\mathbf{D}; \mathbf{z}, \mathbf{X}) \geq 0, \forall j \in \mathcal{F}_D. \\ \text{(ii)} \boldsymbol{\lambda} \geq \mathbf{0}, \\ \text{(iii)} \nabla_{\mathbf{D}} F_0(\mathbf{D}; \mathbf{X}, \mathbf{z}) + \sum_{j \in \mathcal{F}_D} \lambda_j \nabla_{\mathbf{D}} f_j(\mathbf{D}) = \mathbf{0}, \\ \text{(iv)} \lambda_j f_j(\mathbf{D}, \boldsymbol{\lambda}) = 0, \forall j \in \mathcal{F}_D. \end{cases} \quad (35)$$

where (i)-(ii) denote the primal and dual feasibility conditions, (iii) is the stationary condition (i.e., the first-order optimality $\nabla_{\mathbf{X}} L_{\text{AL}} = \mathbf{0}$), and (iv) denotes the complementary slackness conditions. After rearranging the equality constraints in (35), one can obtain the KKT solutions of block variables \mathbf{D} by solving the following system:

$$\boldsymbol{\varphi}(\mathbf{D}, \boldsymbol{\tau}, \boldsymbol{\lambda}, \boldsymbol{\mu}) \triangleq \begin{bmatrix} \nabla_{\mathbf{D}} F_0(\mathbf{D}; \mathbf{X}, \mathbf{z}) + \mathbf{J}_{\mathbf{f}, \mathbf{D}}^T \boldsymbol{\lambda} \\ \text{diag}(\boldsymbol{\lambda}) \mathbf{f}(\mathbf{D}) \end{bmatrix} = \begin{bmatrix} \mathbf{0} \\ \mathbf{0} \end{bmatrix}, \quad (36)$$

where $\mathbf{J}_{\mathbf{f}, \mathbf{D}}^T = [\nabla_{\mathbf{D}} f_1(\mathbf{D}), \nabla_{\mathbf{D}} f_2(\mathbf{D}), \dots, \nabla_{\mathbf{D}} f_{F_D}(\mathbf{D})]$ is the Jacobian matrix of constraint functions $\mathbf{f}(\mathbf{D}; \mathbf{z})$ over \mathbf{D} .

Conventionally, the closed-form KKT solution of \mathbf{D} can be derived when the equality system (36) has a relatively simple structure. The resulting KKT solution of \mathbf{D} would be expressed as a function of the input system parameters \mathbf{z} and the remaining decision variables \mathbf{X} , i.e., $\mathbf{D}^{\text{KKT}} = F^{\text{KKT}}(\boldsymbol{\lambda}, \mathbf{X}, \mathbf{z})$. The key idea of KDL is to **predict dual variables $\boldsymbol{\lambda}$ by learning and directly reconstruct KKT solutions using the data-driven method**. Instead of predicting all primal variables by block-box method or unfolding the computationally-expensive iterative optimization procedure, KDL forces ML to straightforwardly explore the KKT solution structure of \mathbf{D}^{KKT} using

$$\widehat{\mathbf{D}}_{\mathbf{w}}^{\text{KKT}} = F^{\text{KKT}}(\widehat{\boldsymbol{\lambda}}_{\mathbf{w}}(\mathbf{z}), \widehat{\mathbf{X}}_{\mathbf{w}}(\mathbf{z})). \quad (37)$$

Therefore, KDL not only enables the guidance of white-box structure from optimization theory, but also retains the computation efficiency of data-driven and end-to-end learning.

Remark 1: We may not obtain the closed-form solution of all variable blocks in most coupled optimization problem. When conventional optimization algorithm is adopted, the remaining variable block \mathbf{X} that does not have closed-form solution needs to be computed by solving (36) using iterative numerical method, such as interior point method and Newton method [20]. However, this typically requires intensive computations when the number of users/antennas increases. Hence, to maintain a high computation efficiency during execution, KDL will jointly learn the dual variables $\boldsymbol{\lambda}$ and the remaining block variables \mathbf{X} using the data-driven ML model.

2) *KDL Based Joint Transmit Beamforming and Pinching Beamforming*: To apply the proposed KDL paradigm for joint transmit and pinching beamforming optimization, we first provide specific analysis in this part. The KKT solution structure of the original sum rate optimization problem is hard to obtain even using alternative optimization. However, the WMMSE based reformulated problem (P1) provides insights into the KKT solution structure of \mathbf{D} when the remaining variables are fixed, as analyzed as follows. Specifically, the Lagrangian dual function of (P1) can be given by

$$L_{\text{dual}}(\mathbf{D}, \boldsymbol{\lambda}) = \sum_k \alpha_k e_k(\mathbf{X}, \mathbf{D}) + \lambda \left(\sum_k \|\mathbf{d}_k\|^2 - P \right). \quad (38)$$

For ease of notations, the equivalent channels manipulated by pinching beamforming is defined as

$$\widetilde{\mathbf{h}}_k^H(\mathbf{X}) = \mathbf{h}_k^H(\mathbf{X}) \mathbf{G}(x), \quad \forall k \in \mathcal{K}. \quad (39)$$

Using the definition of MSE, i.e., $\sum_{k \in \mathcal{K}} \alpha_k e_k(\mathbf{X}, \mathbf{D}) = \sum_{k \in \mathcal{K}} \alpha_k \left(\sum_{i \in \mathcal{K}} |v_k \widetilde{\mathbf{h}}_k^H(\mathbf{X}) \mathbf{d}_i|^2 + \sigma^2 |v_k|^2 + 1 - 2 \text{Re} \left\{ v_k \widetilde{\mathbf{h}}_k^H(\mathbf{X}) \mathbf{d}_k \right\} \right)$, the first-order optimality condition of $L_{\text{dual}}(\mathbf{D}, \boldsymbol{\lambda})$ w.r.t. \mathbf{d}_k can be expressed as

$$\frac{\partial L_{\text{dual}}}{\partial \mathbf{d}_k} = \sum_{i \in \mathcal{K}} \alpha_i |v_i|^2 \widetilde{\mathbf{h}}_i(\mathbf{X}) \widetilde{\mathbf{h}}_i^H(\mathbf{X}) \mathbf{d}_k - \alpha_k v_k^H \widetilde{\mathbf{h}}_k(\mathbf{X}) + \lambda \mathbf{d}_k = \mathbf{0}, \quad (40)$$

$$\mathbf{d}_k^{\text{KKT}} = \left(\mathbf{I}_N + \sum_i \frac{\alpha_i |v_i|^2}{\lambda} \widetilde{\mathbf{h}}_i(\mathbf{X}) \widetilde{\mathbf{h}}_i^H(\mathbf{X}) \right)^{-1} \frac{\alpha_k v_k^H}{\lambda} \widetilde{\mathbf{h}}_k(\mathbf{X}). \quad (41)$$

Considering the phase rotation equivalency of transmit beamforming \mathbf{d}_k , when we rotate the phase of \mathbf{d}_k into $e^{j\theta} \mathbf{d}_k$, the achievable data rate will not be changed since $\left| \widetilde{\mathbf{h}}_i(\mathbf{X}) \mathbf{d}_k \right|^2 = \left| e^{j\theta} \widetilde{\mathbf{h}}_i(\mathbf{X}) \mathbf{d}_k \right|^2, \forall i \in \mathcal{K}$. Using this property, we can always rotate the phase of $\mathbf{d}_k^{\text{KKT}}$ in (41) to make v_k^H a real and positive value (i.e., $v_k^H = v_k = |v_k|$) without harming the system performance. This means that the KKT solution structure of \mathbf{d}_k can be simplified into

$$\mathbf{d}_k^{\text{KKT}} = \mu_k \left(\mathbf{I}_N + \sum_i \lambda_i \widetilde{\mathbf{h}}_i(\mathbf{X}) \widetilde{\mathbf{h}}_i^H(\mathbf{X}) \right)^{-1} \widetilde{\mathbf{h}}_k(\mathbf{X}), \quad (42)$$

where $\lambda_k = \alpha_k |v_k|^2 / \lambda > 0$ is the weighted dual variable of each user k , and $\mu_k = \lambda_k / v_k$ is a certain (real) scalar that controls the power allocation.

Remark 2: As observed above, the KKT solution of WMMSE-based transmit beamforming optimization shares a highly similar structure with the optimal beamforming structure in [25], which is derived by the KKT solution of a reformulated power minimization problem. This confirms its effectivity from the theoretical aspect.

Based on KDL, we only need to predict dual variables $\lambda = [\lambda_1, \lambda_2, \dots, \lambda_K]$, power allocation coefficients $\mu = [\mu_1, \mu_2, \dots, \mu_K]$, and remaining block variables \mathbf{X} using the ML model $\mathcal{W}(\mathbf{z})$:

$$[\lambda, \mu, \mathbf{X}] = \mathcal{W}(\mathbf{z}), \quad (43)$$

where $\mathbf{z} = [\mathbf{X}^U, \mathbf{y}^U] \in \mathbb{R}^{2K \times 1}$ denotes the vectorized CSI characterized by users' locations, and $\mathcal{W}(\cdot)$ denotes the function of ML model (e.g., deep neural networks). Then, the KKT solution in (42) can be reconstructed by

$$\mathbf{D}^{\text{KKT}} = \text{diag}(\mu) \left(\mathbf{I}_N + \tilde{\mathbf{H}}(\mathbf{X}) \text{diag}(\lambda) \tilde{\mathbf{H}}^H(\mathbf{X}) \right)^{-1} \tilde{\mathbf{H}}(\mathbf{X}), \quad (44)$$

where $\tilde{\mathbf{H}}(\mathbf{X}) \triangleq \mathbf{H}^H(\mathbf{X}) \mathbf{G}(\mathbf{X})$ is the effective channel matrix. In this way, KDL can benefit from both the optimization-guided structure and the iteration-free data-driven learning.

Remark 3: The dimension of output parameters can be reduced by KDL from $N \times K \times 2$ complex transmit beamforming coefficients to only $2K$ dual variables, which enables fast convergence of the learning algorithm.

C. The Proposed KDL-Transformer Algorithm

We implement the proposed KDL based on Transformer, which give rises to a KDL-Transformer algorithm in this part. Specifically, the CSI-to-beamforming optimization problem is regarded as a sequence-to-sequence learning task. The CSI of users is considered as the input sequence, while transmit beamforming and pinching beamforming coefficients are determined using the output sequence. Transformer is known as one of the most core techniques of LLM to model intricate structural data [26], such as nature language, visual, and even multi-modal data. Compared to conventional deep learning techniques, the developed Transformer can capture the long-distance dependence between elements in the input and output sequences. To be more specific, it can dynamically aggregate the context information of PASS by modelling: **(i) inter-PA and inter-user dependencies** that models the spatial distribution and interactions of pinches/users for constructive interference and destructive interference, and **(ii) CSI-beamforming dependencies** that maps various user distributions into efficient transmit and pinching beamforming solutions. By customizing the self-attention and cross-attention mechanisms to learn these relationships, the developed KDL-Transformer algorithm can achieve efficient effective gain enhancement and interference suppression in PASS.

Following existing LLM structure, the developed Transformer consists of a J_E -layer encoder \mathcal{E} and a J_D -layer decoder \mathcal{D} . Compared to vanilla Transformer that exploits masked attention the the decoder, we tailor the Tranformer structure to utilize bidirectional attention mechnisms, thus

modelling global dependence in both the encoder and the decoder: (i) Both the encoder and decoder adopt bidirectional self-attention mechanisms, which characterizes the inter-user dependence in the input sequence and the inter-PA dependence in the output sequence, respectively. (ii) Moreover, the cross-attention mechanism is adopted between the encoder and the decoder to learn the CSI-beamforming dependence, thus refining the transmit bemaforming and pinching beamforming coefficients in correspondence to different CSI. The detailed designs of encoder and decoder are illustrated in the sequel.

1) Encoder Design: The self-attention mechanism of Transformer allows each element (which is also known as *token*) in the sequence to interact with other elements to model their global dependencies. To calculate the attention weights for the vectorized CSI input $\mathbf{z} = [\mathbf{x}^U, \mathbf{y}^U] \in \mathbb{R}^{2K \times 1}$, we need to first embed \mathbf{z} into a high-dimension matrix $\mathbf{Z}_{\text{enc}} \in \mathbb{R}^{2K \times N_{\text{model}}}$, where N_{model} denotes the feature embedding dimension. This can be realized using a learnable linear transform $\mathbf{w}_E \in \mathbb{R}^{N_{\text{model}} \times 1}$ for \mathbf{z} :

$$\mathbf{Z}_{\text{enc}} = \mathbf{z}^T \mathbf{w}_E. \quad (45)$$

The encoder exploits a J_E -layer structure. In each encoding layer, given the embedding feature (i.e., hidden state) \mathbf{Z}_{enc} , Transformer generates three different matrices, named queue \mathbf{Y}_i^Q , key \mathbf{Y}_j^K , and value \mathbf{Y}_j^V . Specifically, queue \mathbf{Y}_i^Q indicates which information requires attentions from the current elements, and key \mathbf{Y}_j^K signifies what information can be provided by each element. Hence, the self-attention score $\mathbf{Y}^Q (\mathbf{Y}^K)^T$ is defined as the inner product of queue and key, which denotes the correlation between elements. Moreover, value \mathbf{Y}_j^V is the representation of the actual information maintained by each element, which will be multiplied with the self-attention score for hidden state update.

We employ multiple attention heads to capture different inter-dependence patterns. Each attention head i individually computes queue, key, and value matrices by

$$\mathbf{Y}_i^K = \mathbf{Z}_{\text{enc}} \mathbf{W}_i^K, \quad \mathbf{Y}_i^Q = \mathbf{Z}_{\text{enc}} \mathbf{W}_i^Q, \quad \mathbf{Y}_i^V = \mathbf{Z}_{\text{enc}} \mathbf{W}_i^V, \quad (46)$$

where I denotes the total number of attention heads, $\mathbf{W}_i^Q, \mathbf{W}_i^K, \mathbf{W}_i^V \in \mathbb{R}^{N_{\text{model}} \times N_{\text{model}}}$ denotes the learnable weight matrices. By normalizing the self-attention scores using the Softmax function and multiplying it with value matrix, each head i obtains the attention weights as follows:

$$\text{head}_i = \text{Attn}(\mathbf{Y}_i^Q, \mathbf{Y}_i^K, \mathbf{Y}_i^V) = \text{softmax} \left(\frac{\mathbf{Y}_i^Q (\mathbf{Y}_i^K)^T}{\sqrt{N_{\text{model}}}} \right) \mathbf{Y}_i^V. \quad (47)$$

Then, the encoder concatenates attention weights from different heads, and computes multi-head features through a learnable matrix \mathbf{W}^O and a feed-forward network (FFN):

$$\text{MultiHead} \left(\left\{ \mathbf{Y}_i^Q \right\}, \left\{ \mathbf{Y}_i^K \right\}, \left\{ \mathbf{Y}_i^V \right\} \right) = \text{FFN} \left(\text{Concat}(\text{head}_1, \text{head}_2, \dots, \text{head}_I) \mathbf{W}^O \right). \quad (48)$$

The hidden state of each encoding layer will be updated based on the multi-head features using a residual connection layer:

$$\mathbf{Z}_{\text{enc}} \leftarrow \mathbf{Z}_{\text{enc}} + \text{MultiHead} \left(\left\{ \mathbf{Y}_i^Q \right\}, \left\{ \mathbf{Y}_i^K \right\}, \left\{ \mathbf{Y}_i^V \right\} \right), \quad (49)$$

which is further used as the input of the next encoding layer.

2) *Decoder Design*: The decoder dynamically attends to relevant information in the final hidden state \mathbf{Z}_{enc} obtained by the encoder, and then predicts primal/dual variables based on a cross-attention mechanism. Let \mathbf{Z}_{dec} denote the prediction of the decoder. At each decoding layer, each attention head i of the decoder generates the key matrix for \mathbf{Z}_{dec} , while computing queue matrix and value matrix using \mathbf{Z}_{enc} :

$$\tilde{\mathbf{Y}}_i^K = \mathbf{Z}_{\text{dec}} \tilde{\mathbf{W}}_i^K, \quad \tilde{\mathbf{Y}}_i^q = \mathbf{Z}_{\text{enc}} \tilde{\mathbf{W}}_i^q, \quad \tilde{\mathbf{Y}}_i^V = \mathbf{Z}_{\text{enc}} \tilde{\mathbf{W}}_i^V. \quad (50)$$

Hence, the cross attention score between \mathbf{Z}_{enc} and \mathbf{Z}_{dec} is obtained by:

$$\text{head}_i = \text{CrAttn}\left(\tilde{\mathbf{Y}}_i^K, \tilde{\mathbf{Y}}_i^q, \tilde{\mathbf{Y}}_i^V\right) = \text{softmax}\left(\frac{\tilde{\mathbf{Y}}_i^q (\tilde{\mathbf{Y}}_i^K)^\top}{\sqrt{N_{\text{model}}}}\right) \tilde{\mathbf{Y}}_i^V. \quad (51)$$

Similar to the encoder, the output is predicted by

$$\mathbf{Z}_{\text{dec}} \leftarrow \mathbf{Z}_{\text{dec}} + \text{MultiHead}\left(\tilde{\mathbf{Y}}_i^K, \tilde{\mathbf{Y}}_i^q, \tilde{\mathbf{Y}}_i^V\right). \quad (52)$$

Algorithm 2 The Proposed KDL-Transformer Algorithm

Input: Vectorized user location (CSI) sequence $\mathbf{z} \in \mathbb{R}^{2K \times 1}$.

Output: Transmit beamforming and pinching beamforming.

Parameters: Model dimension N_{model} , number of heads I , numbers of encoder and decoder layers J_E and J_D

- 1: Compute feature embedding \mathbf{Z}_{enc} by (45).
 - 2: **for** each encoding layer in \mathcal{E} **do**
 - 3: Compute queue \mathbf{Y}_i^Q , key \mathbf{Y}_i^K , and value \mathbf{Y}_i^V for each attention head i by (46).
 - 4: Obtain self-attention by (47) and update \mathbf{Z}_{enc} by (48).
 - 5: **end for**
 - 6: Initialize decoder output by $\mathbf{Z}_{\text{dec}} \leftarrow \mathbf{Z}_{0,\text{out}} + \text{PE}$, where positional encoding $\text{PE}_{(pos, 2i)} = \sin\left(\frac{pos}{10000^{2i/d_{\text{model}}}}\right)$, $\text{PE}_{(pos, 2i+1)} = \cos\left(\frac{pos}{10000^{2i/d_{\text{model}}}}\right)$.
 - 7: **for** each decoding layer in \mathcal{D} **do**
 - 8: Calculate cross attention by (50) and (51).
 - 9: Update \mathbf{Z}_{dec} by (52).
 - 10: **end for**
 - 11: Obtain PA deployment $\mathbf{x}_{\text{end}} \in \mathbb{R}^{N \times 1}$, $\boldsymbol{\omega} \in \mathbb{R}^{N \times L}$, dual variable $\boldsymbol{\lambda} \in \mathbb{R}^{K \times 1}$, and power allocation $\boldsymbol{\mu} \in \mathbb{R}^{K \times 1}$ from $\mathbf{Z}_{\text{dec}} = [\mathbf{x}_{\text{end}}, \boldsymbol{\omega}, \boldsymbol{\lambda}, \boldsymbol{\mu}] \in \mathbb{R}^{(N+M+2K) \times 1}$.
 - 12: Project \mathbf{x}_{end} , $\boldsymbol{\omega}$ by (53), (55) and obtain \mathbf{X} .
 - 13: Construct KKT-conditioned solution \mathbf{D} by (44) and (56).
 - 14: **return** \mathbf{X} , \mathbf{D} .
-

3) *Constraint Guarantees*: We present projection operations in this part to strictly ensure the constraints in (C1) - (C3). First, to satisfy the pinching range limitation (C2), we newly introduce an N -dimension vector $\mathbf{x}^{\text{end}} = [x_1^{\text{end}}, x_2^{\text{end}}, \dots, x_N^{\text{end}}]$ that assigns the positions of the last PA along each waveguide. Therefore, we can simply project \mathbf{x}^{end} into feasible region $L\Delta_{\min} \leq \mathbf{x}^{\text{end}} \leq S_{\text{PA}}$ using

$$\mathbf{x}^{\text{end}} \leftarrow L\Delta_{\min} + \text{Sigmoid}(\mathbf{x}^{\text{end}})(S_{\text{PA}} - L\Delta_{\min}), \quad (53)$$

where $\text{Sigmoid}(\cdot)$ is the Sigmoid activation function. To simultaneously guarantee the minimum spacing constraint (C1),

we further predict the spacing $\boldsymbol{\omega}_n^T = [\omega_{n,1}, \omega_{n,2}, \dots, \omega_{n,L}] \in \mathbb{R}^{1 \times L}$ between any two PAs along the n -th waveguide. Specifically, $\omega_{n,1}$ denotes the distance from the first PA $l = 1$ to the feed point of each waveguide n , and $\omega_{n,l} = x_{n,l} - x_{n,l-1}$, $\forall l \geq 1$, indicates the mutual intervals between the remaining PAs. We introduce the following operation to guarantee the minimum spacing constraint (C1). Given a threshold $0 < \epsilon \leq 1/L$ and a positive vector $\mathbf{z} = [z_1, z_2, \dots, z_L]$, $0 \leq z_l \leq 1$, the projection operation

$$\mathbf{z}_{\text{proj}} = \mathcal{P}(\mathbf{z}, \epsilon) = \epsilon + \frac{1 - L\epsilon}{\sum_{l=1}^L z_l} \mathbf{z} \quad (54)$$

ensures that $\mathbf{z}_{\text{proj}} \geq \epsilon$ and $\sum_{l=1}^L z_{\text{proj},l} = 1$. Therefore, we can ensure the minimum spacing constraints using

$$\boldsymbol{\omega}_n \leftarrow x_n^{\text{end}} \mathcal{P}\left(\boldsymbol{\omega}_n, \frac{\Delta_{\min}}{x_n^{\text{end}}}\right), \quad \forall n \in \mathcal{N}. \quad (55)$$

As a result, the position $x_{n,l}$ of the l -th PA at waveguide n can be obtained by accumulating the intervals of previous l PAs using $x_{n,l} = \sum_{i=1}^l \omega_{n,i}$, $\forall l \in \mathcal{L}$, $\forall n \in \mathcal{N}$.

Moreover, we ensure the transmitting power constraint (C3) by projecting μ_k into range $[0, P]$ and normalizing \mathbf{D} using

$$\mu_k \leftarrow \frac{\mu_k P}{\sum_{i \in \mathcal{K}} \mu_i}, \quad \mathbf{D}^{\text{KKT}} \leftarrow \frac{\mathbf{D}^{\text{KKT}} \text{diag}(\boldsymbol{\mu}^{1/2})}{\sum_{i \in \mathcal{K}} \|\mathbf{d}_i^{\text{KKT}}\|^2}. \quad (56)$$

Algorithm 2 summarizes the computation procedure for the developed KDL-Transformer algorithm for predicting solutions. Based on the proposed structure, the encoder and the decoder will be jointly trained through end-to-end learning to minimize the loss function, i.e., the negative system sum rate.

V. SIMULATION RESULT

In this section, we provide numerical results to demonstrate the effectiveness of the proposed PASS design and algorithms, where a BS serves $K = \{4, 6\}$ single-antenna users in downlink MIMO communications. The system operates at $f = 30$ GHz frequency band, and the wavelength is $\lambda_f = 0.01$ meters. Users are randomly distributed in a range of $S_x \times S_y = 20 \times 10$ m² area. Both users and PASS have fixed heights, where $z_k^U = 0$, $\forall k \in \mathcal{K}$, and $h_{\text{PA}} = 2.5$ meter, $\forall n \in \mathcal{N}$. To ensure multiplexing gains, the number of RF chains used by PASS is set as $N = K$. Each RF chain is connected to a waveguide, and each waveguide has $L = \{8, 12, 16, 20, 24, 28, 32\}$ PAs. All the waveguides stretch across a span of 20 meters along the x -axis (horizontal) direction. Moreover, the waveguides are uniformly spaced along the y -axis (vertical) directions with an equal interval of $d_W = S_y/N$ meter. The maximum transmission power is set as $P = \{10, 12, 14, 16, 18, 20, 22, 24\}$ dBm, and the noise power is $\sigma^2 = -90$ dBm. The refraction index is given by $n_{\text{eff}} = 1.4$. The residual tolerance for the termination of MM-PDD algorithm is set as $\epsilon = 10^{-6}$, and the initial penalty factor is $\rho^{(0)} = 10^{-4}$. We generate 30000 samples by Monte-Carlo simulation to train KDL-Transformer, and generate a test dataset of 64 samples for each simulation setting to compare the performance of the KDL-Transformer and the MM-PDD algorithms. Several baseline algorithms are considered:

- **Massive MIMO (PDD):** The conventional massive MIMO array based on hybrid beamforming architecture [28] is adopted at the BS located at the origin point, where PDD algorithm [27] is utilized to jointly optimize the analog beamforming and the transmit beamforming. Aligned with the proposed PASS, the massive MIMO uses a sub-connected structure, where each RF chain is only connected to a subset of L antennas through L phase shifters, thus reducing the hardware costs and complexity.
- **Black-box Transformer/ResNet:** The end-to-end unsupervised learning is adopted, which trains a black-box Transformer and a 50-layer ResNet for joint transmit and pinching beamforming, respectively.
- **KDL-ResNet:** The proposed KDL is implemented by training a 50-layer ResNet model.
- **KDL-Transformer without cross attention (KDL-Transformer-OCA):** The proposed KDL is implemented by training a self-attention Transformer that does not involve the cross-attention mechanism.

Fig. 2 demonstrates the convergence behaviors of the developed MM-PDD algorithm in terms of both the achievable system sum rate and the maximum constraint residual, i.e., $\|\mathbf{B}\|_\infty$. As shown in Fig. 2, by appropriately initializing the penalty factor ρ , the developed MM-PDD algorithm can successfully seek the directions to increase the system sum rate and reduce the constraint residuals simultaneously. Specifically, the maximum constraint residuals $\|\mathbf{B}\|_\infty$ rapidly decreases within the first 40 iterations. As the punishments on constraint residuals become small, the achievable system sum rate will dramatically enhance and finally achieve convergence. At the convergence, the constraint residual eventually approach 0 and becomes stable, which implies that the equality constraints can be satisfied at convergence. When different numbers of PAs L are activated along each waveguide, the developed MM-PDD algorithm can reach convergence within 50 iterations, which verifies its efficiency. Furthermore, when L increases, the convergence speed would not be decreased, as the punishments on equation violation increase with L , which will enforce PAs to quickly determine their locations.

Fig. 3 exhibits the convergence behaviors of the proposed KDL-Transformer algorithm and other learning algorithms, where the eventual performance achieved by MM-PDD algorithm is also displayed for comparisons. The detailed numerical results are further presented in Table I. As shown in Fig. 3, the black-box learning algorithms based on both ResNet and Transformer perform much worse than the MM-PDD algorithm. This is because the coupled beamforming optimization problem has numerous local optimums and saddle points, making it difficult for the unsupervised learning to seek high-quality solutions by solely relying on gradient

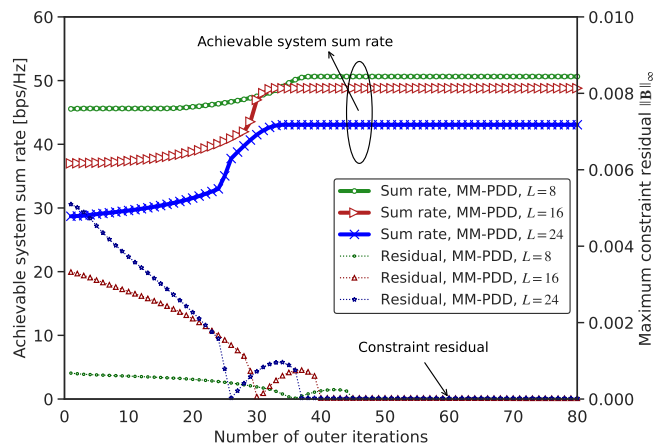


Fig. 2: Convergence behaviors of the developed MM-PDD algorithm. $K = 4$, $P = 10$ dBm, $S_x = 20$ m.

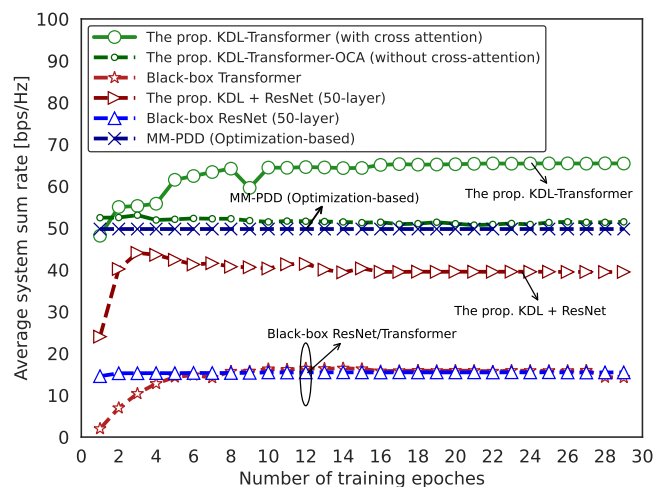


Fig. 3: Comparisons of convergence performance of the proposed KDL-Transformer with other learning-based algorithms. $K = 4$, $L = 8$, $P = 10$ dBm, $S_x = 20$ m.

descent. By contrast, despite the utilized ML models, the proposed KDL method can significantly enhance the performance of learning-based algorithms, which confirms its efficiency to approximate KKT points. Notably, the proposed KDL-Transformer algorithm improves over 30% performance than the MM-PDD algorithm. This demonstrates its potentials to circumvent the inefficiency of iterative alternating block descent required by the optimization algorithms. Furthermore, the proposed KDL-Transformer improves over 40% and over 20% performance than *KDL-ResNet* and *KDL-Transformer-OCA*, which confirms that its efficiency in characterizing both inter-PA/inter-user and CSI-beamforming dependencies.

Fig. 4 shows the system performance of different algorithms

TABLE I: Detailed comparisons of numerical results over NVIDIA A40 workstation.

Performance	Method	MM-PDD ($\rho = 0.01$)	KDL-Transformer (with cross attn.)	KDL-Transformer-OCA (without cross attn.)	KDL-ResNet (50 layers)	Black-box Transformer (without cross attn.)	Black-box ResNet (50 layers)	Conventional MIMO (WMMSE-PDD)
Sum rate ($K = 4, L = 8$)		49.76	65.83	<u>55.61</u>	43.03	15.99	16.46	32.14
Execution time (second)		255.51/sample	0.0324/batch	0.0277/batch	<u>0.0172/batch</u>	0.0196/batch	0.0157/batch	157.21/sample
Sum rate ($K = 4, L = 16$)		47.20	67.68	<u>53.01</u>	45.58	16.71	16.75	28.54
Execution time (second)		408.12/sample	0.0477/batch	0.0436/batch	0.0201/batch	0.0198/batch	0.0198/batch	179.24

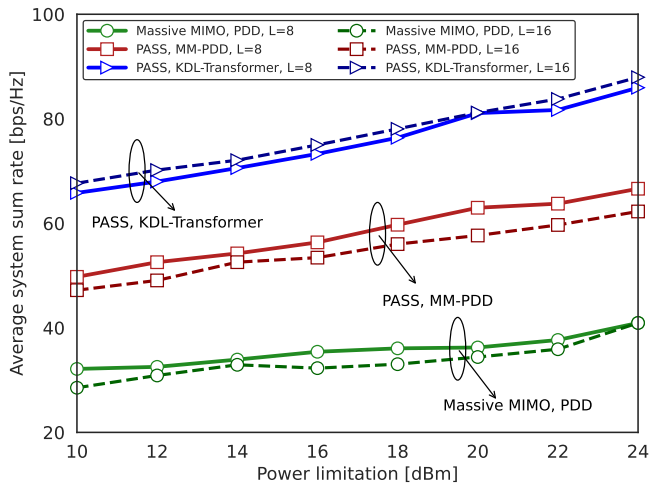


Fig. 4: Performance comparisons of different algorithms under different P . $K = 4$, $S_x = 20$ m.

under various transmitting power limitations P . The system sum rates of both the conventional massive MIMO and the proposed PASS framework increase with P . Both the MM-PDD algorithm and the KDL-Transformer algorithm significantly improve the system sum rate compared to the conventional massive MIMO architecture, which confirms the efficiency of the proposed PASS architecture in reconfiguring large-scale path loss and spatial multiplexing for MISO communications. Moreover, the developed KDL-Transformer algorithm achieves the highest system performance, and the achieved performance gain increases with P , which demonstrates its potential to enhance the resource utilization efficiency.

Fig. 5 compares the system sum rates of different approaches when different numbers of pinches/antennas are activated on each waveguide/RF chain. Specifically, the system sum rates of both massive MIMO and PASS increase with the number of associated users K , which confirms their effectivity in spatial multiplexing. Nevertheless, as the number of activated antennas L increases, the performance of both the massive MIMO and the MM-PDD algorithm deteriorates due to increased mutual interference. By contrast, the performance achieved by KDL-Transformer algorithm may be improved with a larger number of activated pinches. This implies that the optimization-based algorithms may prematurely fall into local optimums, but the pinching beamforming solutions learnt by KDL-Transformer can explore more efficient interference suppression, thus leveraging the pinching deployment agility when more PAs are activated.

Fig. 6 further demonstrates the performance of different approaches when spatial range S_x varies from 5 m to 25 m. It can be observed that the system performance of conventional massive MIMO degrades as the spatial range increases, especially when the transmission power budget is small. In comparison, the performance of the developed MM-PDD algorithm slightly changes as the spatial range increases, since PASS can avoid the long-distance path loss experienced by conventional MIMO. Furthermore, the developed KDL-Transformer consistently outperforms both MM-PDD and conventional massive MIMO, but the performance decreases with the spatial ranges.

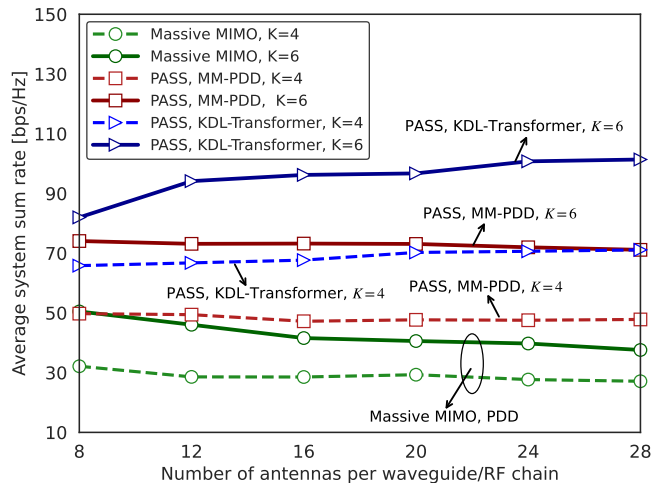


Fig. 5: Comparisons of average sum rate of the proposed algorithms under different L . $P = 10$ dBm, $S_x = 20$ m.

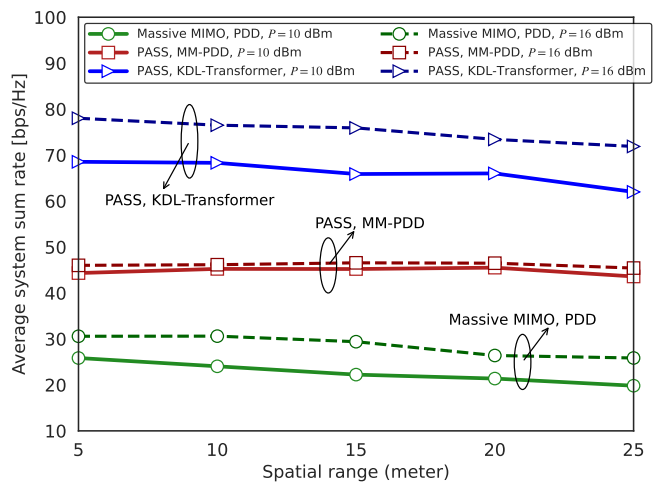


Fig. 6: Comparisons of average sum rate of the proposed algorithms under different spatial ranges S_x . $K = 4$, $L = 8$.

This may be because when the spatial range of user distributions enlarges, the distribution of PAs also becomes more sparse, which will decrease the overall array gains.

VI. CONCLUSION

A novel PASS-enabled multi-user MISO framework has been proposed, which enables pinching beamforming to adjust both large-scale path loss and phases of radiated signals. A joint transmit and pinching beamforming optimization problem was formulated to maximize the system sum rate. To tackle this highly coupled and nonconvex problem, both optimization-based and learning-based methods have been proposed. The optimization-based method, named MM-PDD algorithm, used a convex surrogate function to handle complex exponential components and invoked PDD for problem decoupling, which was guaranteed to obtain stationary solutions. The learning-based method, termed KDL-Transformer, directly reconstructed KKT-conditioned solutions in a low-complexity and data-driven way, where the underlying inter-PA/inter-user and CSI-beamforming dependencies were effectively learned

by Transformer. Numerical results have been provided to verify the efficiency of both the proposed PASS framework and algorithms. In future, the design of joint transmit and pinching beamforming under imperfect CSI can be further investigated.

APPENDIX

A. Proof of Lemma 1

The WMMSE problem w.r.t. v_k can be written as

$$\min_{\{v_k\}} \sum_k \alpha_k J_k |v_k|^2 - 2\alpha_k \text{Re} \{v_k \mathbf{h}_k^H(\mathbf{X}) \mathbf{G}(\mathbf{X}) \mathbf{d}_k\}. \quad (57)$$

Using the first-order optimality, the equalizer of MMSE receiver v_k^{opt} can be obtained by (13). Substituting (13) into (11), the MSE e_k^{MSE} is rewritten as

$$e_k^{\text{MSE}} = (1 - \mathbf{d}_k^H \mathbf{G}_k^H(\mathbf{X}) \mathbf{h}_k(\mathbf{X}) J_k^{-1} \mathbf{h}_k^H(\mathbf{X}) \mathbf{G}(\mathbf{X}) \mathbf{d}_k). \quad (58)$$

Then, the objective function in (P1) becomes convex with respect to α_k . By fixing the remaining variables, we have

$$\alpha_k^{\text{opt}} = (1 - \mathbf{d}_k^H \mathbf{G}_k^H(\mathbf{X}) \mathbf{h}_k(\mathbf{X}) J_k^{-1} \mathbf{h}_k^H(\mathbf{X}) \mathbf{G}(\mathbf{X}) \mathbf{d}_k)^{-1} = (e_k^{\text{MSE}})^{-1}. \quad (59)$$

Substituting α_k^{opt} and v_k^{opt} into (12a), problem (P1) becomes

$$\max_{\mathbf{x}, \mathbf{D}} \sum_{k=1}^K \left(\log_2 (e_k^{\text{MSE}})^{-1} \right), \quad \text{s.t. (C1) - (C3)}. \quad (60)$$

Combining $(e_k^{\text{MSE}})^{-1} = E_k / \left(\sum_{k' \neq k} I_{kk'} + \sigma^2 \right) = 1 + \text{SINR}_k$, (60) is equivalent to (P0), which ends the proof.

B. Proof of Lemma 2

The complex number c can be written as $c = |c|e^{-i\phi_c}$. Using Euler formula $e^{i\theta} = \cos(\theta) + i \sin(\theta)$, we can rewrite function $-\text{Re}(ce^{i(a\theta)})$ into

$$f(\theta) = -\text{Re} \left\{ ce^{i(a\theta)} \right\} = -|c| \text{Re} \left\{ e^{i(a\theta - \phi_c)} \right\} = -|c| \cos(a\theta - \phi_c). \quad (61)$$

Hence, the first-order and the second-order derivatives of $f(\theta)$ can be given by

$$\nabla_{\theta} f(\theta) = a|c| \sin(a\theta - \phi_c), \quad \nabla_{\theta}^2 f(\theta) = a^2|c| \cos(a\theta - \phi_c). \quad (62)$$

Since $|\cos(a\theta - \phi_c)| \leq 1$, the second-order gradient is upper bounded. According to the mean value theorem, the gradient of $f(\theta)$ is Lipschitz continuous, i.e.,

$$\begin{aligned} \|\nabla_{\theta} f(\theta_1) - \nabla_{\theta} f(\theta_2)\| &\leq \left(\max_{\theta \in [\theta_1, \theta_2]} |\nabla_{\theta}^2 f(\theta)| \right) \|\theta_1 - \theta_2\| \\ &\leq a^2 |c| \|\theta_1 - \theta_2\|, \quad \forall \theta_1, \theta_2 \in \mathbb{R}. \end{aligned} \quad (63)$$

Hence, the Lipschitz gradient constant is given by $\varrho^{\theta} = \max_{\theta} |\nabla_{\theta}^2 f(\theta)| = a^2 |c|$, which ends the proof.

REFERENCES

- [1] C. E. Shannon, "A mathematical theory of communication," *Bell Syst. Tech. J.*, vol. 27, no. 3, pp. 379-423, Jul. 1948.
- [2] M. Di Renzo et al., "Smart radio environments empowered by reconfigurable intelligent surfaces: How it works, state of research, and the road ahead," *IEEE J. Sel. Areas Commun.*, vol. 38, no. 11, pp. 2450-2525, 2020.
- [3] X. Mu, Y. Liu, L. Guo, J. Lin and R. Schober, "Simultaneously Transmitting and Reflecting (STAR) RIS Aided Wireless Communications," *IEEE Trans. Wireless Commun.*, vol. 21, no. 5, pp. 3083-3098, May 2022.
- [4] K.-K. Wong, A. Shojaefard, K.-F. Tong, and Y. Zhang, "Fluid antenna systems," *IEEE Trans. Wireless Commun.*, vol. 20, no. 3, pp. 1950-1962, Mar. 2021.
- [5] L. Zhu, W. Ma, and R. Zhang, "Modeling and performance analysis for movable antenna enabled wireless communications," *IEEE Trans. Wireless Commun.*, vol. 23, no. 6, pp. 6234-6250, Jun.
- [6] Z. Ding, R. Schober, H. V. Poor, "Flexible-antenna systems: A pinching-antenna perspective," *arxiv*, arXiv:2501.10753, 2025.
- [7] Y. Liu, Z. Wang, X. Mu, C. Ouyang, X. Xu, and Z. Ding, "Pinching Antenna Systems (PASS): Architecture Designs, Opportunities, and Outlook," *arXiv preprint*, arXiv 2501.18409, 2025.
- [8] H. O. Y. Suzuki and K. Kawai, "Pinching antenna - using a dielectric waveguide as an Antenna," *NTT DOCOMO Technical Journal*, vol. 23, no. 3, pp. 5-12, Jan. 2022.
- [9] Y. Xu, Z. Ding, G. K. Karagiannidis, "Rate Maximization for Downlink Pinching-Antenna Systems," *preprint*, 2025.
- [10] C. Ouyang, Z. Wang, Y. Liu, and Z. Ding, "Array gain for pinching-antenna systems (PASS)," *arXiv preprint*, arXiv: 2501.05657, 2025.
- [11] K. Wang, Z. Ding, and R. Schober, "Antenna Activation for NOMA Assisted Pinching-Antenna Systems," *arXiv preprint* arXiv:2412.13969, Dec. 2024.
- [12] H. Elayan, O. Amin, B. Shihada, R. M. Shubair, and M. Alouini, "Terahertz band: The last piece of RF spectrum puzzle for communication systems," *IEEE Open J. Commun. Society*, vol. 1, pp. 1-32, Nov. 2020.
- [13] H. Zhang, N. Shlezinger, F. Guidi, D. Dardari, M. F. Imani, and Y. C. Eldar, "Beam focusing for near-field multiuser MIMO communications," *IEEE Trans. Wireless Commun.*, vol. 21, no. 9, pp. 7476-7490, Sept. 2022.
- [14] D. M. Pozar, *Microwave engineering: theory and techniques*, John Wiley & sons, 2021.
- [15] Q. Shi, M. Razaviyayn, Z. -Q. Luo and C. He, "An Iteratively Weighted MMSE Approach to Distributed Sum-Utility Maximization for a MIMO Interfering Broadcast Channel," *IEEE Trans. Signal Process.*, vol. 59, no. 9, pp. 4331-4340, Sept. 2011.
- [16] A. L. Yuille and A. Rangarajan, "The concave-convex procedure (CCCP)," in *Proc. Adv. Neural Inf. Process. Syst.*, 2002, vol. 2, pp. 1033-1040.
- [17] Y. Sun, P. Babu and D. P. Palomar, "Majorization-Minimization Algorithms in Signal Processing, Communications, and Machine Learning," *IEEE Trans. Signal Process.*, vol. 65, no. 3, pp. 794-816, Feb. 1, 2017.
- [18] Y. Xu and W. Yin, "A block coordinate descent method for regularized multiconvex optimization with applications to nonnegative tensor factorization and completion," *SIAM J. Imaging Sci.*, vol. 6, no. 3, pp. 1758-1789, 2013.
- [19] Q. Shi and M. Hong, "Penalty Dual Decomposition Method for Nonsmooth Nonconvex Optimization—Part I: Algorithms and Convergence Analysis," *IEEE Trans. Signal Process.*, vol. 68, pp. 4108-4122, 2020.
- [20] F. A. Potra and S. J. Wright, "Interior-point methods," *J. Comput. Appl. Math.*, vol. 124, no. 1-2, pp. 281-302, 2000.
- [21] T. Chen, X. Chen, W. Chen, H. Heaton, J. Liu, Z. Wang, and W. Yin, "Learning to Optimize: A Primer and A Benchmark," *J. Mach. Learn. Res.*, vol. 23, no. 189, pp. 1-59, 2022.
- [22] A. Balatsoukas-Stimming and C. Studer, "Deep Unfolding for Communications Systems: A Survey and Some New Directions," *Proc. IEEE Int. Workshop Signal Process. Syst. (SiPS)*, Nanjing, China, Oct. 2019, pp. 266-271.
- [23] Q. Hu, Y. Cai, Q. Shi, K. Xu, G. Yu and Z. Ding, "Iterative Algorithm Induced Deep-Unfolding Neural Networks: Precoding Design for Multiuser MIMO Systems," *IEEE Trans. Wireless Commun.*, vol. 20, no. 2, pp. 1394-1410, Feb. 2021.
- [24] S. Boyd and L. Vandenberghe, *Convex Optimization*, Cambridge, U.K.: Cambridge Univ. Press, 2004.
- [25] E. Björnson, M. Bengtsson and B. Ottersten, "Optimal Multiuser Transmit Beamforming: A Difficult Problem with a Simple Solution Structure [Lecture Notes]," *IEEE Signal Process. Mag.*, vol. 31, no. 4, pp. 142-148, Jul. 2014.
- [26] A. Vaswani, N. Shazeer, N. Parmar, J. Uszkoreit, L. Jones, A. N. Gomez, L. Kaiser, and I. Polosukhin, "Attention is all you need," in *Proc. Adv. Neural Inf. Process. Syst. (NeurIPS)*, Long Beach, CA, USA, Dec. 2017, pp. 5998-6008.
- [27] Q. Shi and M. Hong, "Spectral Efficiency Optimization for Millimeter Wave Multiuser MIMO Systems," *IEEE Trans. Signal Process.*, vol. 66, no. 11, pp. 2944-2958, June 2018.
- [28] X. Song, T. Kühne and G. Caire, "Fully-/Partially-Connected Hybrid Beamforming Architectures for mmWave MU-MIMO," *IEEE Trans. Wireless Commun.*, vol. 19, no. 3, pp. 1754-1769, Mar. 2020.